Bottom Drag Meter

Design & Construction of an Instrument to Allow for Comparison Measurements of Shear Stress on Sediments Resulting From the Propagation of Waves Produced By Jet Skis

by

Terri Gentes
Department of Civil Engineering
Undergraduate Ocean Research

Report Submitted on April 23, 1999

UNHMP-TR-SG-99-4

Sea Grant
New Hampshire/Maine

Acknowledgement

I would to express my sincere appreciation to those who have helped with this project. Glen Rice worked on this project from September and his role in helping design an adequate data acquisition process was very important. His ability to work around our vastly different schedules, especially during testing, was much appreciated.

I would also like to thank my advisor Dr. Franz Anderson. His technical support as well as his good humor kept Glen and I interested and making progress.

Robert Champlain, in the machine shop, was a tremendous help with this project. He guided me through the construction of this project. He was adamant that I learn as much as possible about each corner of the machine shop and despite my initial lack of knowledge was willing to take the time to do that. Wally Fournier also was instrumental in completing this project as well.

John Scott was very helpful with the budget especially concerning the purchase of materials.

Finally I would like to thank the graduate students in the Ocean Engineering building. Both Rob Steen and Dave Fredrickson took time out of their busy schedules on several occasions to offer advice or technical support to us.

This work is the result of research sponsored in part, by the National Sea Grant College Program, NOAA, Department of Commerce, under grant #NA76RG0084 through the University of New Hampshire/University of Maine Sea Grant College Program.

ABSTRACT

Jet Skis have the ability to produce relatively large amplitude waves in shallow waters that are normally protected from wave action. As these waves propagate forward they impart part of their energy to the bottom sediments. This shearing action may result in erosion and increased turbidity within the water column. An instrument was constructed to serve as one component of a study being conducted in the summer of 1999 by Dr. Franz Anderson at the University of New Hampshire. The objective of the instrument is to provide an easily recorded measurement of shearing stress that can be used for comparison purpose.

An instrument was designed and constructed that measures the shear stresses resulting from particle interaction with a moveable plate. To increase the signal resulting from small stresses, an attempt was made to increase particle interaction by coating various plates with different size aggregates. The instrument was calibrated and tested in a tow tank. The results of the tow-tests showed that increases in shear stress were observed with increases in velocity. It also showed a direct relationship between particle size and shear stress. However, some limitations and uncertainty existed especially at low speeds.

For particle speeds greater than 1 ft/sec the instrument appears to be somewhat reliable and useful for analysis in the field.

TABLE OF CONTENTS

LISTS OF FIGURES

LISTS OF TABLES

BACKGROUND

Personal watercraft vehicles, also known by Kawasaki Motors Corporation trade name "Jet Skis" are typically designed with a 110 horsepower, 2-stroke engine that allows them to achieve speeds of 60 miles per hour (Williams, 1998). Jet skis do not have propellers; thus, they can travel at these high speeds even in extremely shallow water and their slender size makes almost any narrow inlet or bay accessible. These characteristics, as wells as there comparatively affordable price, have had a positive impact to the 1.4 billion-dollar Jet Ski industry whose sales last year were the highest of all the recreational watercraft sectors. However, the increased operation of Jet Skis has had many environmentalist, scientists, and legislatures concerned.

Like other two-stroke engines, fuel consisting of gas and oil is inefficiently burned and as much as 25% is released into the water during operation (Gorant, 1998). California is combating these increased emissions by imposing strict regulations and supporting the development of new craft with more efficient fuel injection systems.

The operation of jet skis near shore also causes the formation of erosive waves and excessive noise levels. The combinations of these effects have been observed to have negative impacts on the surrounding wildlife. The Anti-Jet Ski Association was established in San Juan County, Washington after citizens of Puget Sound observed the rapid decrease in wildlife activity after heavy Jet Ski traffic (Williams, 1998). Jonna Burger of Rutgers University has studied shoreline-nesting foul for twenty years. In the past two years, she reports, "almost total nesting failure and an enormous increase in Jet Ski traffic" (Williams, 1998). There is similar concern in New Hampshire, particularly

for the welfare of Loons (Gavia immer) who build their nests on the water's edge and will sometimes abandon eggs after a single disturbance (William, 1998).

There has also been concern expressed that Jet Skis operated at high speeds in shallow waters will lead to bank erosion and sediment transport. Passing waves induce a shearing stress on the bottom sediments that may cause sediment transport or particle suspension in the water column. After the wave passes, these particles settle out of water at vary rates.

In many cases, estuarine environments naturally protected from high currents and wave action are not protected from Jet Ski traffic. In Hampton NH, citizens, local fisherman, and scientist expressed their concern over illegal use of Jet Skis within fragile salt marshes and pleaded for stricter enforcement of the state's law, which prohibit individuals from operating watercraft within 150 feet of the shore. David Goethel, a fisherman and local biologist reported Jet Skis "cause erosion along the salt marsh banks and pollution" (Sharkey, 1998).

To evaluate the impacts of wave propagation resulting from Jet Ski action, Dr. Franz Anderson at the University of New Hampshire, will conduct a study beginning in the summer of 1999. He will look, specifically, at the association between Jet Ski waves and increases in estuarine turbidity. Since waves, induce a shearing stress on the bottom sediments, an instrument was designed and constructed to attempt to evaluate the shearing stress in the field.

INTRODUCTION

Motorized watercrafts produce waves as they travel through water. Jet Skis, particularly, have the ability to produce relatively large amplitude waves in shallow water. At a particular water depth the wave motion begins to interact with the bottom sediments, imparting some energy. The tangential stress on the sediments due to this interaction has been termed the shearing stress.

Wave Theory

A widely accepted mathematical theory that describes wave propagation in shallow waters is the Solitary Wave Theory derived by J. Boussinesq in 1972 (Dean: Dalyrmple, 14). Anderson used Solitary Wave Theory in this 1975 study on suspended sediment concentrations resulting from the passage of a boat wave. Michallet and Barthelemy believed shoreward propagation of solitary waves were responsible for nutrient mixing (Michallet; Barthelemy, 1998).

Solitary waves are progressive waves whose motion is unaffected by receding or following crests. Unlike linear waves, solitary waves do not have troughs. The theory assumes horizontal velocity of water particles below the crest of the wave. It doesn't account for a boundary layer. A boundary layer is a layer of mixing particle velocities formed when a moving fluid particle encounters a stationary object. Water particles within the boundary layer move slower than the free-stream velocity (Roberson; Crowe, 1997). Figure 1 shows the parameters used in solitary wave theory.

The celerity, c, is the speed of the wave propagation as is represented by equation 1. Water particle velocity, u, beneath the crest of a wave is given in equation 2. The depth, z, is measured from the bottom sediments ($z = 0$ at the soil/water interface). The maximum velocity, which occurs when $z = 0$, is shown in Equation 3.

Figure 1: Reference Diagram for Solitary Wave Theory

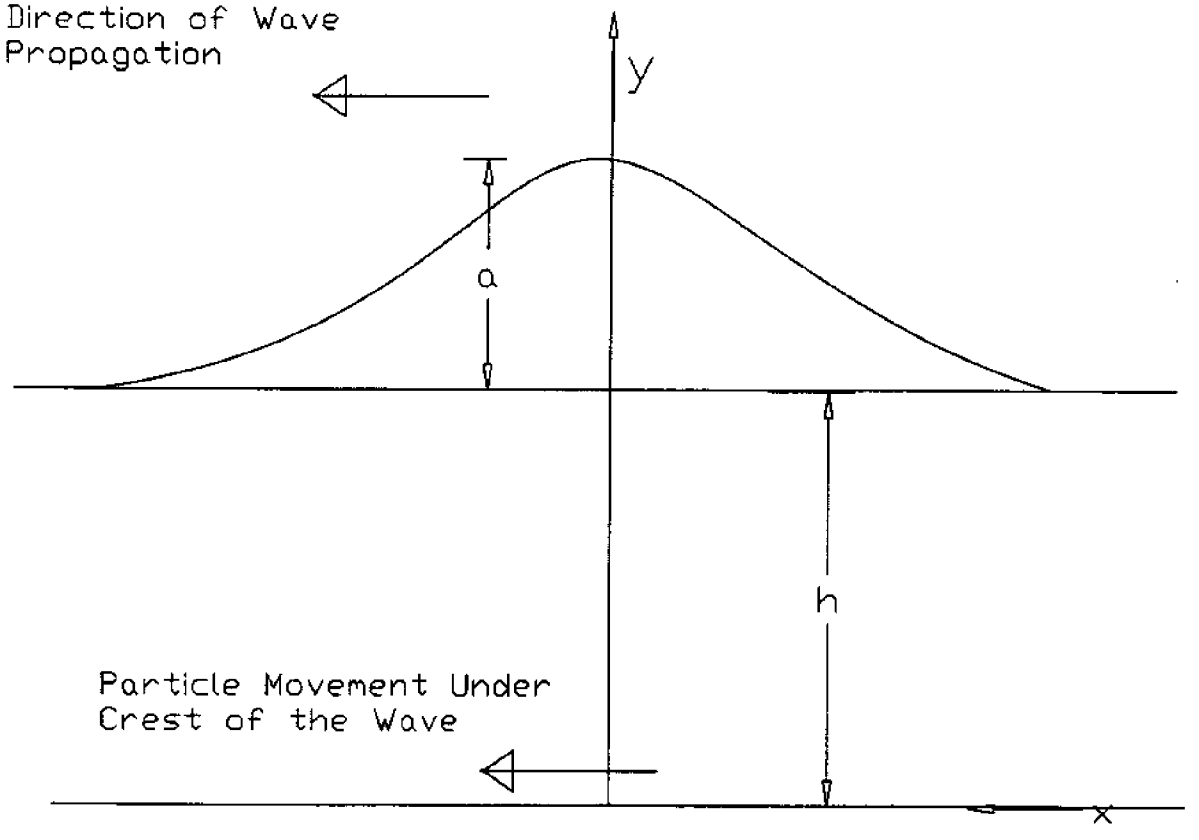

Equation 1

$$c = \sqrt{g \cdot h} \cdot \left(1 + \frac{a}{2 \cdot h}\right)$$

Where c = celerity, g= gravity, a = wave amplitude, h = ambient water depth

Equation 2

$$u = c \cdot \left[\frac{a}{h} \cdot \left[1 + \frac{a}{4 \cdot h} \cdot \left[3 \cdot \left(\frac{z}{h}\right)^2 - 5\right]\right]\right]$$

Where u = maximum particle velocity under the crest of the wave at location z, a = wave amplitude, h = ambient water depth, and z = water depth measured from the bottom sediments upward

Equation 3

$$u = c \cdot \frac{a}{h} \cdot \left(1 + \frac{a}{4 \cdot h} - 5\right)$$

Where u = maximum particle velocity under the crest of the wave when z = 0.

Shear Stress Analysis

The local shear stress resulting from moving fluid interacting with a fixed plate is given in Equation 4. The generic form of this equation has also been used to evaluate the shearing stress in due to solitary wave interaction with particle sediments (See Myrhaug, et al, 1998). The overall shear force on a smooth plate is obtained by integration the local stress over the area of the plate (See equation 5). In this equation, the friction factor *f* is represented by C_f, an empirically determined factor that is based on Prandt's Mixing Length Theory for turbulent flow over a completely smooth plate (Roberson, Crowe).

Equation 4

$$\tau_o = f \cdot \frac{u^2}{2} \cdot \rho$$

where

τ_o = shearing stress (lb/ft^2)
f = friction factor
u = free stream velocity(ft/sec)
ρ = density of fluid ($slugs/ft^3$)

Equation 5

$$F_d := \frac{u^2}{2} \cdot B \cdot L \cdot \rho \cdot C_f$$

Where:
B = Width of the Plate (ft)
L = Length of Plate (ft)
ρ = Density (1.99 slugs/ft^3)
C_f = friction factor
U = free stream velocity (ft/sec)

Equation 6

$$C_f := \frac{.074}{Re_{max}^{\frac{1}{5}}}$$

Where :

$$Re_{max} := \frac{u \cdot L}{\nu}$$

And

Re_{max} = Reynolds Number (Dimensionless Parameter)
u = maximum particle velocity under the crest of the wave (ft/sec)
L = Length of the Plate (ft)
ν = kinematic viscosity (ft^2/sec)

In natural environments, the friction coefficient, *f*, is dependent upon a variety of factors. Schlichting showed that for flat plates *f* is dependent upon the type of flow: laminar or turbulent (Roberson: Crowe, 1997). Turbulent flow is defined as flow that contains mixing zones and eddies. Generally, in naturally moving bodies of water, the flow near the bed can be considered turbulent (Myrhaug et al, 1998). Moody showed a direct relationship between the relative roughness of sand-coated pipes and the friction coefficient (Roberson: Crowe, 1997). Relative roughness is defined as the sand particle diameter divided by the diameter of the pipe.

Studies have been done empirically determine a value for the coefficient of friction that is relevant to bottom friction beneath water waves. For instance, Soulsby et

al. (1993a) proposed a relationship for the coefficient of friction for sinusoidal waves based on empirical data (Myrhaug, 1995). It is $f = c(A/z_o)^{-d}$, where A is orbital displacement, z_o is the seabed roughness parameter, and *c* & d are constants.

Myrhaug, et al. attempted to relate theoretical models for bottom shearing stress caused by random waves to estimates of stress composed of experimentally determined parameters. These parameters included velocity near the seabed, suspended sample concentrations, seabed configurations (ripples), and seabed sediment samples. The theoretical models were based upon simple eddy viscosity models and Prandtl's mixing length models. Myrhaug found "significant differences in the agreement between predicted and estimated values of shear stress." He later proposed a complex method for determining *f* that is based on wave parameters, sediment parameters, sediment suspension rates and complex statistical analysis.

Due to the complexity and uncertainty in determine a suitable friction coefficient, *f*, an attempt is made to measure the shear stress directly by this instrument. The values obtained from the instrument will be used for comparison purpose and will not represent the actual shearing stress on sediments.

Wave Modeling Based on Solitary Wave Theory

Boussinesq equation was used to predict wave velocities that were likely to be observed in field studies. Reasonable assumptions were made concerning the depths of water where observations would be taken as well as the expected amplitudes and are shown in Table 1. Ambient water conditions were assumed to remain stable and large currents were neglected. Amplitudes greater than 25% of the ambient water depth were not used in analysis to ensure accurate predictions of velocity. The ranges of velocities expected are shown in figures 2 and 3.

Table 1: Expected Field Conditions: Assumptions of Water Depth and Wave Amplitude

Water Depth, h	1.8 to 4.8 feet
Amplitude, a	0.1 to 0.9 feet

Figure 2: Range of Celerities Expected in Field Approximated by Solitary Wave Theory (Celerity is given on vertical axis in feet/second.)

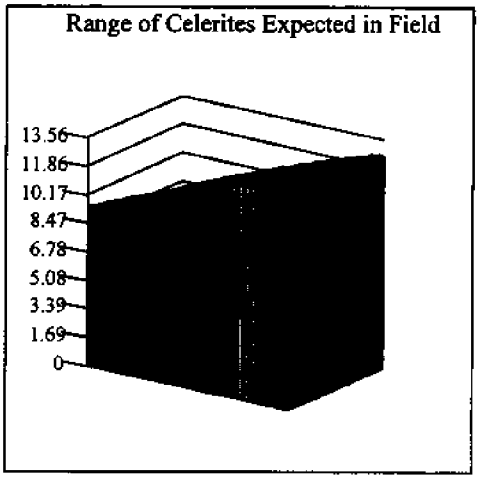

c

Figure 3: Expected Range of Maximum Velocities, u, Under the Crest of the Wave Approximated by Solitary Wave Theory (Velocity is on the axis in feet/second)

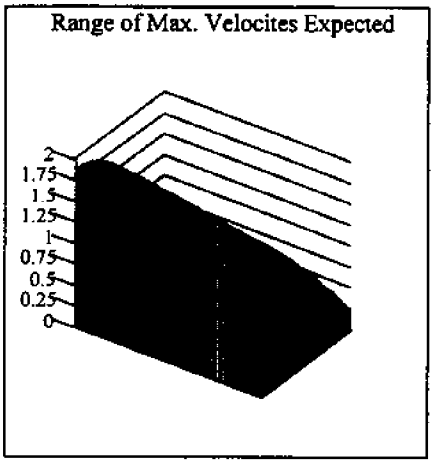

u

Instrumental Design

The design of the instrument was based on a set of criteria set forth at the beginning of the project.

Design Criteria

Ability to Meet Objectives

1. The instrument must measure shearing stress directly and produce a signal that can be easily recorded
2. The data obtained in the field must be easy to read and analyze.
3. The instrument must be reliable and should have an estimated life span of 1 year or more.
4. The instrument must be able to identify and measure the small stresses that are expected in the field. Ideally, the instrument would distinguish small changes in shearing stress caused by the Jet Ski wave despite large background stresses such as large currents.
5. The instrument should be able to measure shearing stress just above the boundary layer. Due to the non-linearity of stress near the seabed it is undesirable to extrapolate readings that are obtained at locations far above the seabed.
6. The instrument should cause as little disruption as possible to the natural sediments and to the water column.

Ability to Withstand Environmental Conditions

1. The instrument must withstand the corrosive properties of salt water.
2. The instrument must withstand a temperature regime of 32°F to approximately 80°F.
2. Effects from water pressure must be considered in the design.

External Constraints

1. Construction limitations - The instrument must be constructed at the University of New Hampshire. Limitations do exist concerning the knowledge and ability of metalworking.
2. Monetary Constraints - Although adequate money was provided, the best instrument would be as economical as possible. Care would also be taken to ensure that money was available for repairs or other mishaps.

The selected instrument consists of two major components: The physical structure and the data acquisition system. Figure 4 shows the completed instrument.

Physical description

The instrument basically consists of a heavy aluminum base plate, a lightweight top plate, and four supporting legs machined from thin brass (See Figures 5 and 6). The top plate is allowed to move in the horizontal direction both forward and backward. The legs are attached to both the bottom and top plate. They are completely fixed to the bottom plate by the use of two screws in order to prevent rotational movement of the legs.

Moving the top plate results in the formation of moments in each leg. Moments produce stresses and the subsequent deformation of the legs. A useful term relating this deformation is strain (the change in length over the initial length ($\Delta L/L$)). The relationship between moments and strain is shown by equation 7.

Equation 7

$M = \varepsilon * E * A * x$

where: ε = strain
E= Modulus of Elasticity
x = distance from applied force to strain gage
A = area of the top plate

Figure 4: Bottom Drag Meter

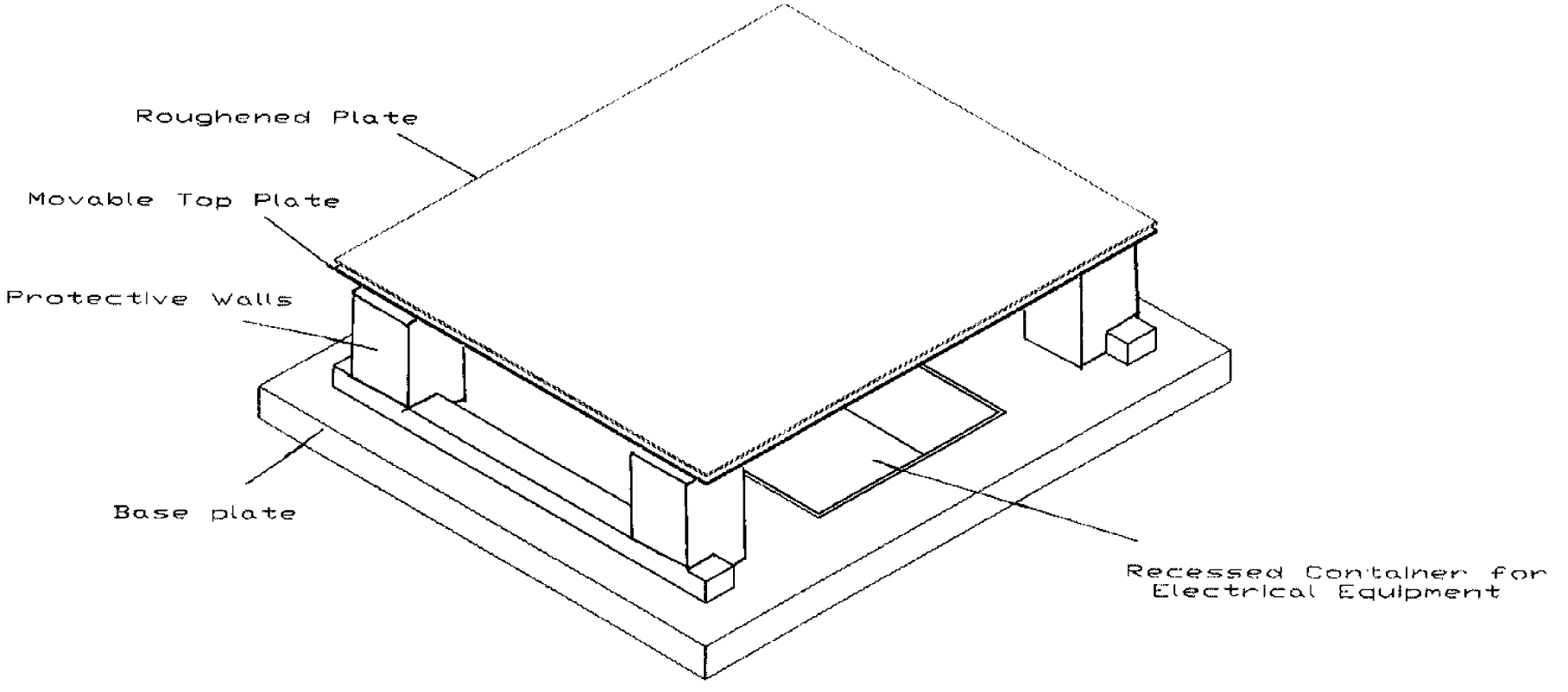

Figure 5: Bottom Drag Meter

Shown without Protective Legs

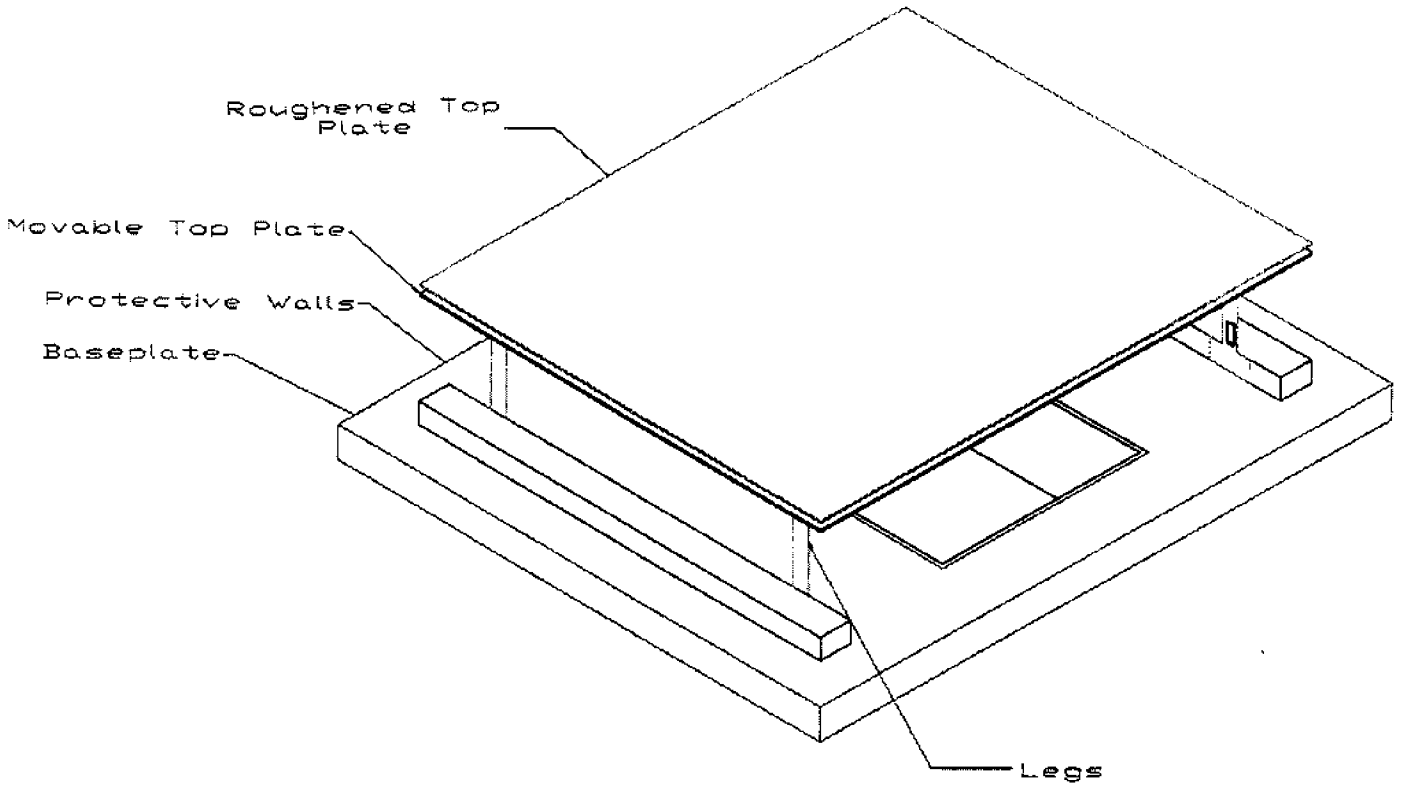

Figure 6: Brass Legs of Bottom Drag Meter with Strain Gages Attached

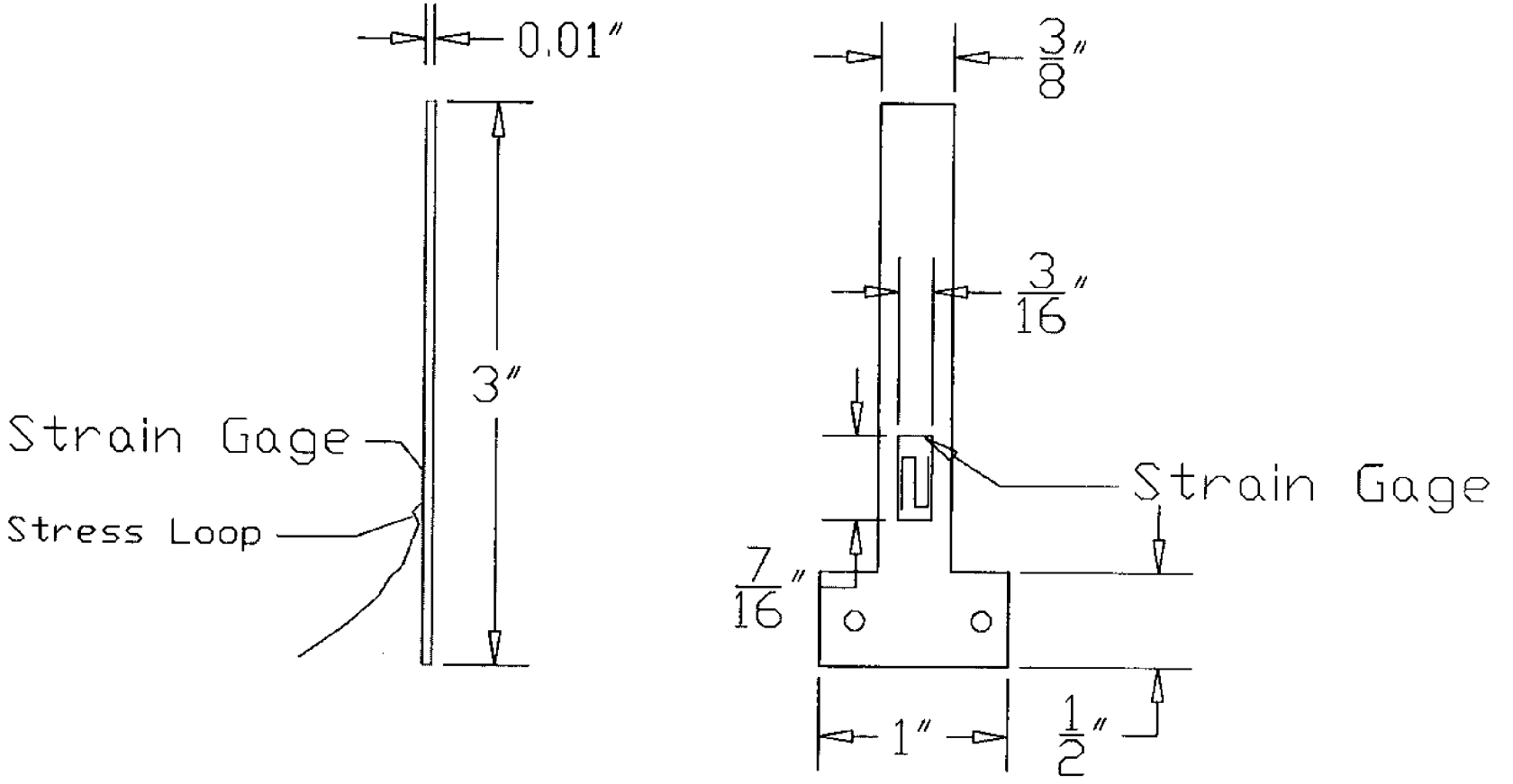

Strain is measured by using strain gages that are mounted the legs. The maximum moment occurs close to the fixed end of the legs. The moment extremely close to the fixed support is difficult to analyze, thus, to ensure good readings, the center of each gage is located 0.5 inches from the fixed support. The following section on data acquisition describes the process of acquiring data from the gages.

The strain gages were purchased from Vishay MicroMeasurements. The gages selected were model 250UW. The gages were adhered to each leg and protected using a waterproof sealant. A more detailed description of the procedure can be found in the Appendix. Three wires extend from each gage and are threaded through a sealed hole in a waterproof box. The waterproof box contains the voltage source, data logger, and amplifier, such that the instrument is self-contained with no wires extending to the surface. Data is recorded and stored, without disruption, for a period of 1.5 hours.

Materials were selected for the project based upon their ability to withstand the corrosive properties of salt water. All components are aluminum or brass and all hardware is stainless steel. The waterproof box was purchased from Otterbox Incorporated and was thoroughly tested before any electrical equipment was placed inside of it.

The size of the legs and size of the top plate are the only controllable factors that determine the amount of strain that will be observed. The equation below shows this relationship for a smooth plate:

Equation 8

$$\varepsilon := 6 \cdot \frac{\frac{F_d}{4} \cdot x}{E \cdot b \cdot w^2}$$

Where F_d = Drag Force, x = Distance from Applied force to gage, b = width of leg, w = thickness of leg, and ε = strain.

For most materials, strain is proportional to stress over a certain region and all deformations are elastic or non-permanent. To prevent permanent deformation it is necessary to ensure that the strain in the legs and gages is within the elastic range for strain gages of +/- 3% strain or 0.03 in/in. Various leg dimensions were analyzed using equation 8 to ensure the strain would be significantly less than 3%. The optimum leg sizes were selected to meet these criteria and to minimize the distance from the top plate to the bottom plate.

Shearing stress, the parameter of interest, acts in a horizontal direction opposing the motion of flow and causes movement of the top plate. To ensure that only this movement would produce stress in the legs, four protective boxes were constructed around each leg. The size of these boxes was selected to allow both full movement of each leg without interference and to prevent disruption of the flow path.

The total height from the top plate to the based of the second plate is 3.75 inches. If readings closer to the bed are desired the instrument can be buried in the sediment. Four walls, 2.5 inches high surround the instrument and provide stability and further gage protection. To prevent flow disruption, these walls should be removed if the instrument is not buried.

A holder within the base plate was constructed so that the top of the waterproof box is at the same elevation as the base plate. This was done to minimize the creation of eddies, mixing zones, between plates that would cause inaccurate movement of the top plate.

Water pressure acts on all submersed bodies equally on all faces of the object. By allowing a clear flow path beneath the top plate and bottom plate, the resulting water pressure on the top plate will be zero. Thus, water pressure effects will not interfere with the readings.

To increase the friction factor, three plates were constructed that can be added to

the top plate. The plates were coated with sand grains by using a marine epoxy. The average effective diameter of the sand particles was determined by sifting aggregates using US Standard sieves. The openings of the sieves used are 0.221 in, 0.131 inches, 0.055 inches, and 0.028 inches. The average diameters on each plate are shown in table 2 below.

Table 2: Average Size of Aggregates Attached to Each Plate

Smooth Plate	No Coating
Plate 1	0.0415 Inches
Plate 2	0.0930 Inches
Plate 3	0.0176 Inches

Data Acquisition

The goal of the data acquisition system was to provide a way to easily obtain meaningful data that can be directly related to shear stress. It consists of three major components: The Wheatstone Bridge, a Differential Amplifier, and a Data Logger. An overall schematic of this system is shown in Figure 7.

Description of Wheatstone Bridge

A strain gage is a grid configuration of an extremely small wire that is bonded to a flexible plastic backing. All gages are produced using a precise process of photoetching that allows for the production of identical gages. When they are properly adhered to test specimens they experience the almost same deformations or strains, as the test specimen. To measure this deformation, or strain, a constant voltage can be applied across the gages, which function as resistors. The resistance is proportional the to the strain. For instance, a gage adhered to a test specimen experiencing tension also is placed in tension.

Figure 7: Complete Data Acquisition System for Bottom Drag Meter Instrument

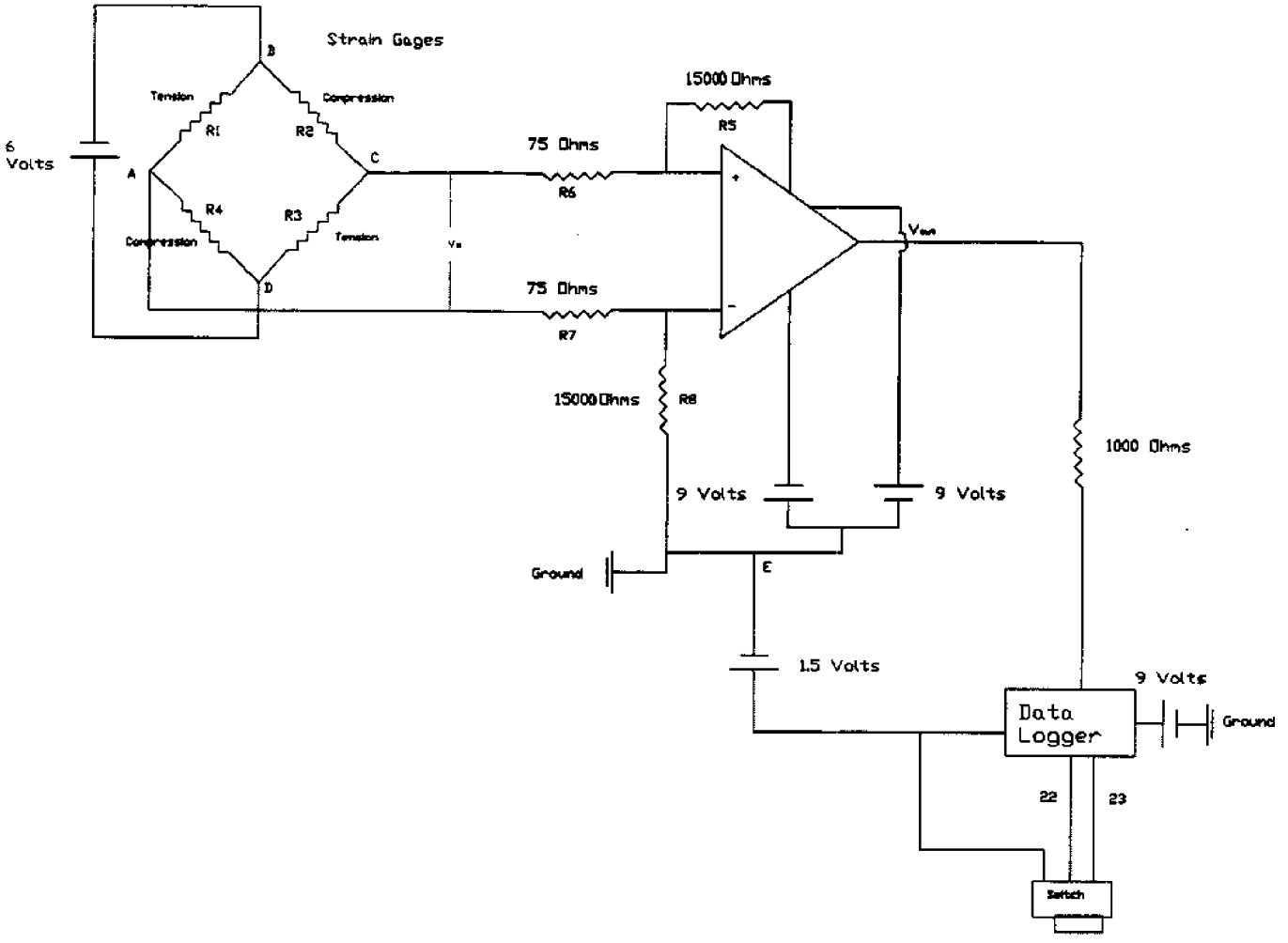

The wire length increases and so the total resistance of the gage increases. Ohm's Law states that a change in resistance is proportional to the change in voltage. Thus by measuring the voltage leaving the resistor an idea of the strain experienced by the resistor and test specimen.

A commonly used circuit in strain gage analysis is the Wheatstone Bridge. It requires at least four resistors or gages. Three variations of the Wheatstone Bridge exist. A full bridge occurs when all four gages are connected to the test specimen, a half bridge utilizes two gages, and a quarter bridge requires only one gage to be connected to the specimen. The quarter and half-bridge configurations require dummy gage and fixed-resistance gages to complete the circuit. The dummy gage serves to cancel voltage outputs that are due to temperature fluctuations or differences in temperature between the test specimen and the internal fixed resistant gages. It must be placed on a stress-free location of the test specimen that is located in the same thermal environment as the active gage. In generally, the full-bridge configuration offer several advantages over the half and quarters bridge configurations including larger outputs and eliminates the need for dummy gages and fixed resistant gages.

A diagram of the full-bridge configuration is shown in Figure 8. The voltage output is determined by assessing the top and bottom parts of the bridge as individual voltage dividers. The output voltage, v_o, is measured at nodes B and D and is equal to v_{BD} or v_{AB}-v_{AD}. The output voltage can also be assessed in terms of input voltage, v_s, and individual gage resistance, R_1,R_2,R_3,R_4. The equation below shows this relationship.

Output Voltage

$$v_o = v_s(R_1R_3 - R_2R_4 /((R_1+R_2)(R_3+R_4)))$$

Figure 8: Wheatstone Bridge Configuration

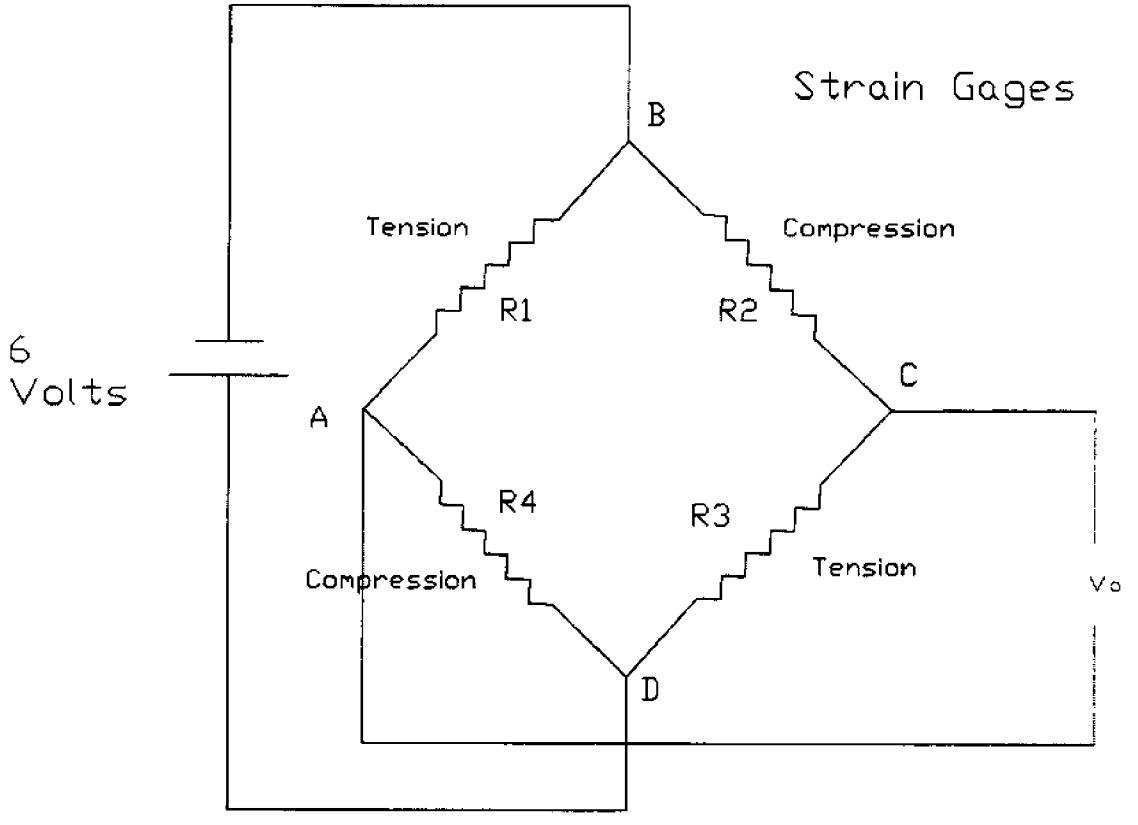

When R_1R_3 & R_2R_4 is equal to zero, the bridge is balanced. If the bridge is balanced when the specimen or structure is in equilibrium, the change in voltage, Δv_o, can be measured when a force or pressure is applied. Several advantages exist to this method. First, it is not necessary to subtract output reading from an initial value. Also for dynamic loading, it is generally much easier to distinguish small changes in voltage when the actual voltage readings are small. It is more difficult to isolate milli-volt changes from initial large voltages. To balance the bridge, Resistor 1 and Resistor 3 should be situated at some location on the specimen where they are experiencing the same strain. Resistor 2 and Resistor 4 should also be placed at a location where their strain is equal and opposite from R_1 & R_3.

To utilize the full bridge on this instrument each leg on the instrument contained one gage situated on its inside portion as shown in Figure 6. The gages were installed along the center axis and were located 2.25 inches from the top plate.

The bridge was completed using the circuit shown in Figure 8. Horizontal motion of the top plate results in equal strain in gages 1 and 3. Meanwhile, gages 4 and 2 experience strain of equal magnitude, but opposite in direction. In Figure 8a, gages 1 and 3 are shown to be in tension and 2 and 4 are shown to be in compression. The bridge is balanced when no external forces are applied to the plate. Six volts, in the form of 4 – 1.5 volt batteries (AA), function as the voltage supply for the bridge through a switch.

Differential Amplifier

The output lines from the Wheatstone bridge circuit are connected to a differential amplifier that functions to increase the output signal from the bridge to a readable form

Figure 8a: Full Wheatstone Bridge Configuration - Wiring Diagram

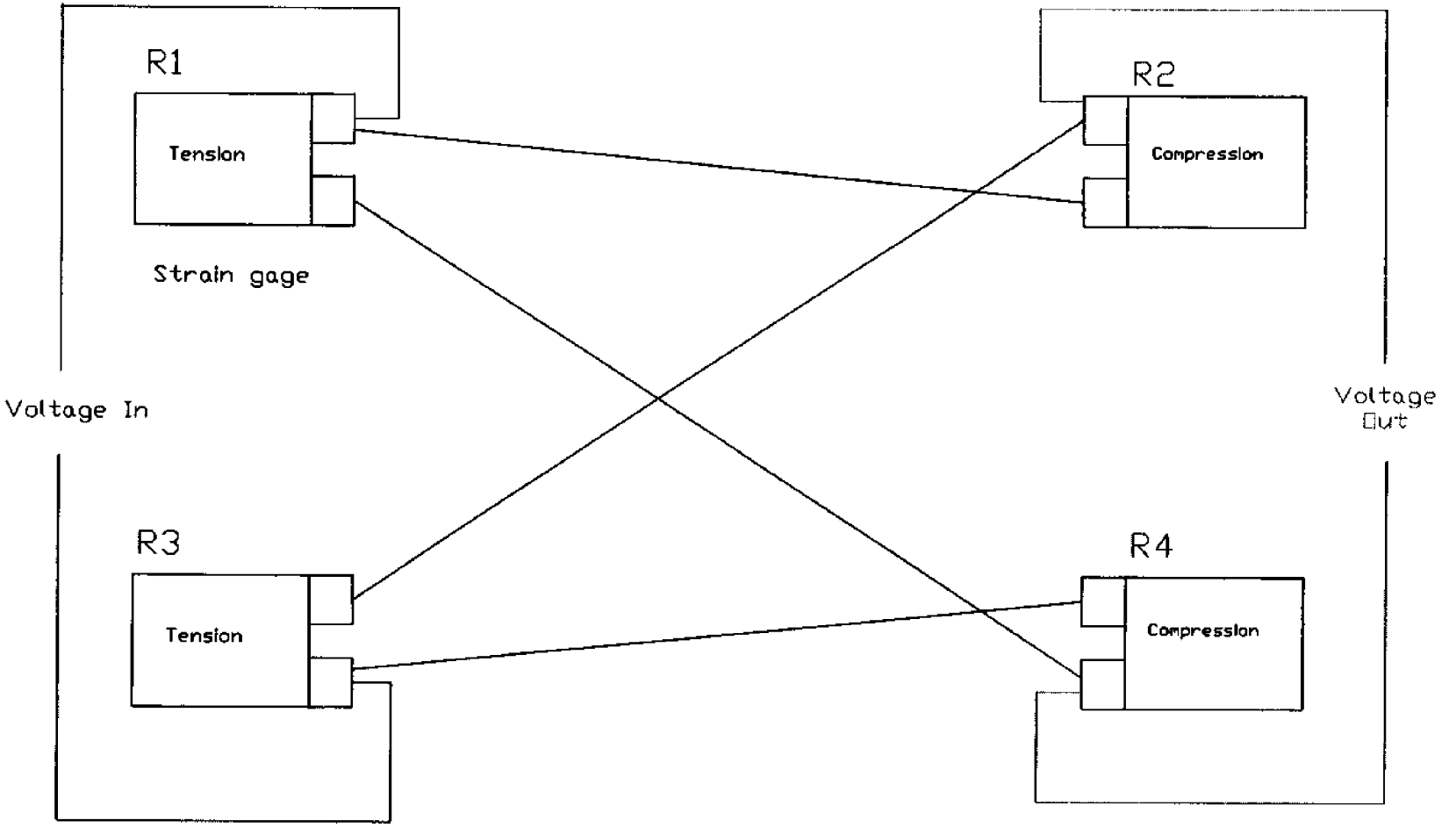

The input voltage, v_{in}, to the amplifier is the voltage potential output measured at nodes B and D. A schematic of the amplifier is shown in Figure 10. The amplifier is constructed of an FET Op-amp and resistors from radioshack. The differential amplifier requires a power supply as shown by the two 9 – volt batteries, where ground for the output of the amplifier is between the + 9 and –9 voltage supplies.

To ensure that the output from the amplifier is zero when the input voltage from the bridge, $v_{in,}$ is equal to zero, an biasing circuit was established. This circuit consists of resistors labeled 5, 6, 7, and 8 in the diagram. The biasing circuit in combination with the operational amplifier forms a differential amplifier. The gain of the system is equivalent to the ratio of v_{in}/v_{out} and is equivalent to R_5/R_6 or 20.

Forward and backward motion of the top plate results in strain readings that are can be either positive or negative. For purposes of data recording and computer analysis, this was not desirable. To alleviate this problem, ground for the data logger was connected to a 1.5 volt battery (node E), thereby moving the voltage change to positive at all times (See Figure 7).

The Data Logger

A remote data logger, model TFX-11, was purchased from Onset Computer Corporation to record data while in the field. This allows the instrument to be self-contained and eliminates the need for extension of external wires to the water's surface.

The output voltage from the amplifier was passed through a 1000-ohm resistor and then to the data logger as shown in Diagram 10. Onset Computer Corporation recommended the addition of the 1000-ohm resistor to prevent the data logger from being shocked by unexpectedly or sudden large voltage readings. Operation of the data logger

Figure 9: Differential Amplifier

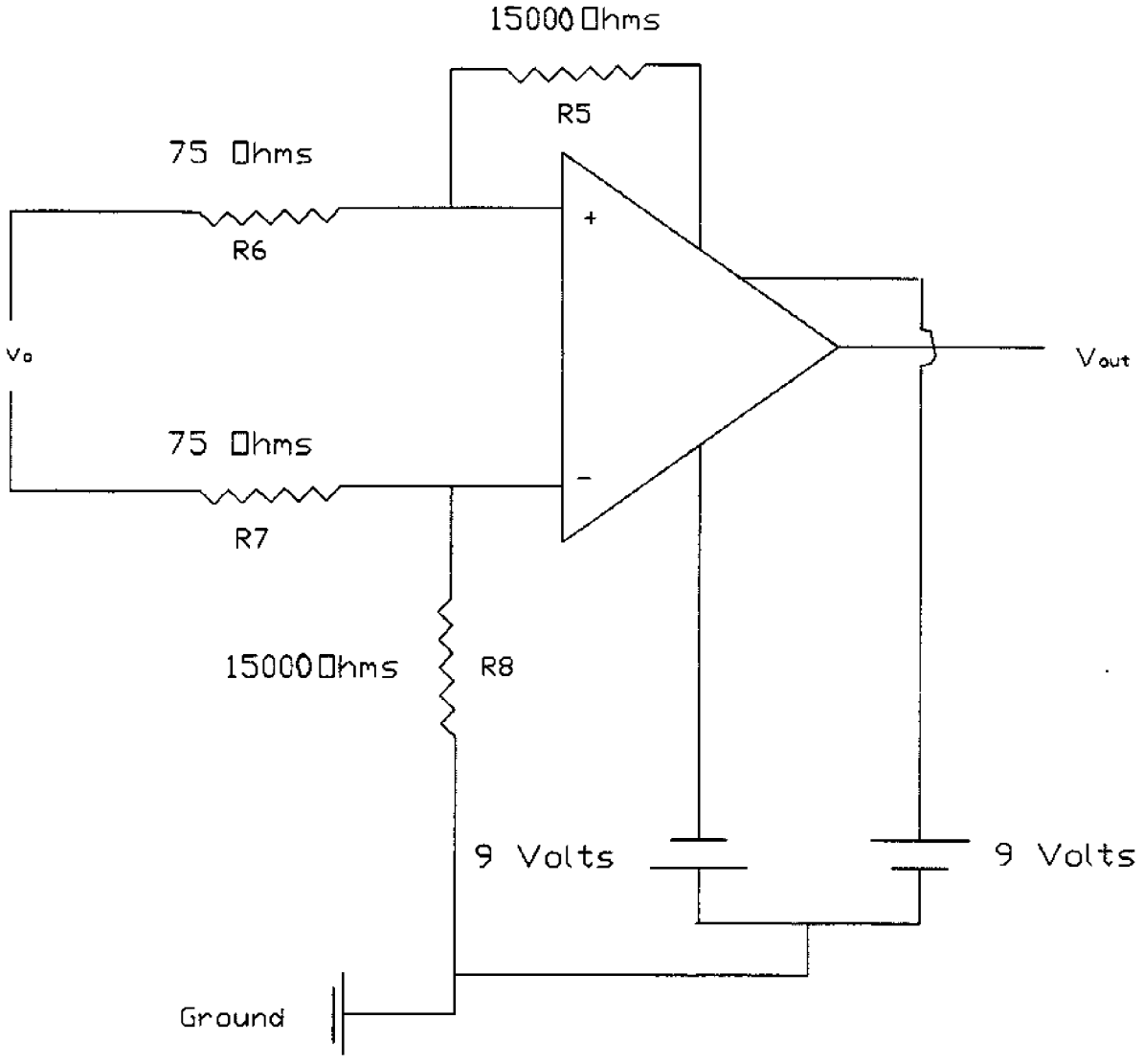

requires a 9-volt battery that is connected to a ground. A switch was installed to allow the user to tell the data logger to begin recording data, and to shut off. When the switch is in the on position the data logger reads +5 volts from the switch (location 22), and 0 volts when the switch is off

The sampling rate of the data logger can be selected based upon the individual operator's discretion and can be as low as 0.01 samples per second. During the testing procedure, the sampling rate was selected at .1 samples per second. A program was established to set the sampling time and define the sampling procedure. The first part of the program checks to see if someone has manually turned on the data logger. The second part of the program orders the data logger to record and store values received from the amplifier. The complete program is given in the Appendix.

CALIBRATION

The instrument was calibrated so that measurements of voltage recorded in the field could be easily translated to values of shear stress. Figure 10 is a schematic of the calibration procedure. Known values of mass were strung from the top plate and over a low-friction pulley. Under the force gravity, these masses produced a shearing force on the top plate. The data acquisition system was used to obtain voltage reading for each force applied. These forces were translated into values of shearing stress by dividing by the area of the top plate.

The individual values of mass used in calibration are shown in Table 4. A calibration curve was plotted to shown the relationship between shearing stress and voltage readings. A linear regression was used to obtain an equation which best fit the data. The equation is:

$$\text{Shearing Stress } (lb/ft^2) = 0.0014 + 0.0004 * \text{Change in Voltage (millivolts)}$$

Table 3: Masses Used in Calibration Process of Bottom Drag Meter
(Calibration was conducted on April 14, 1999)

Mass (grams)	Force (pounds)
0	0.008
3.8	0.013
5.8	0.019
13.8	0.030
23.8	0.052
53.8	0.119
103.8	0.229
128.8	0.284
163.8	0.361

Figure 10: Diagram Showing Calibration setup and Procedure

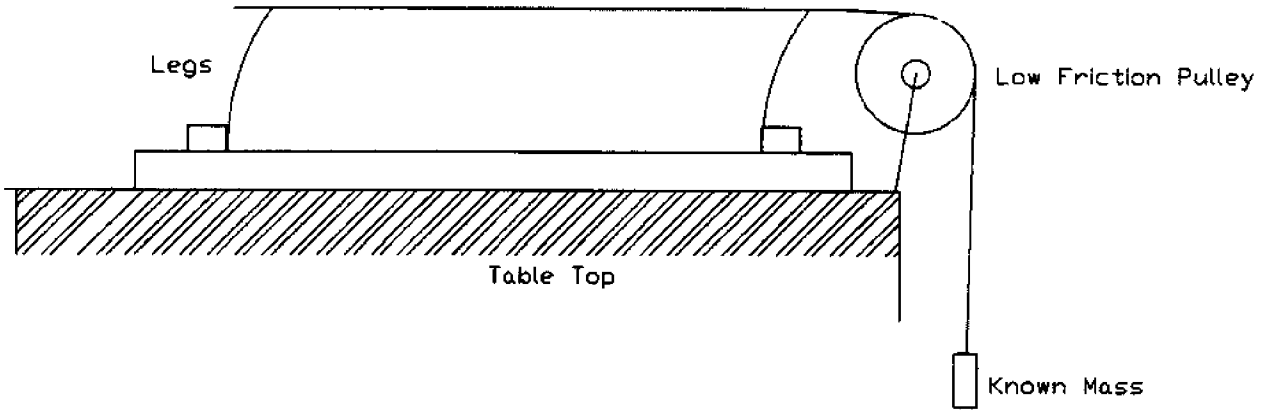

Figure 11:Calibration Curve for Bottom Drag Meter

(Data obtained on April 16, 1999)

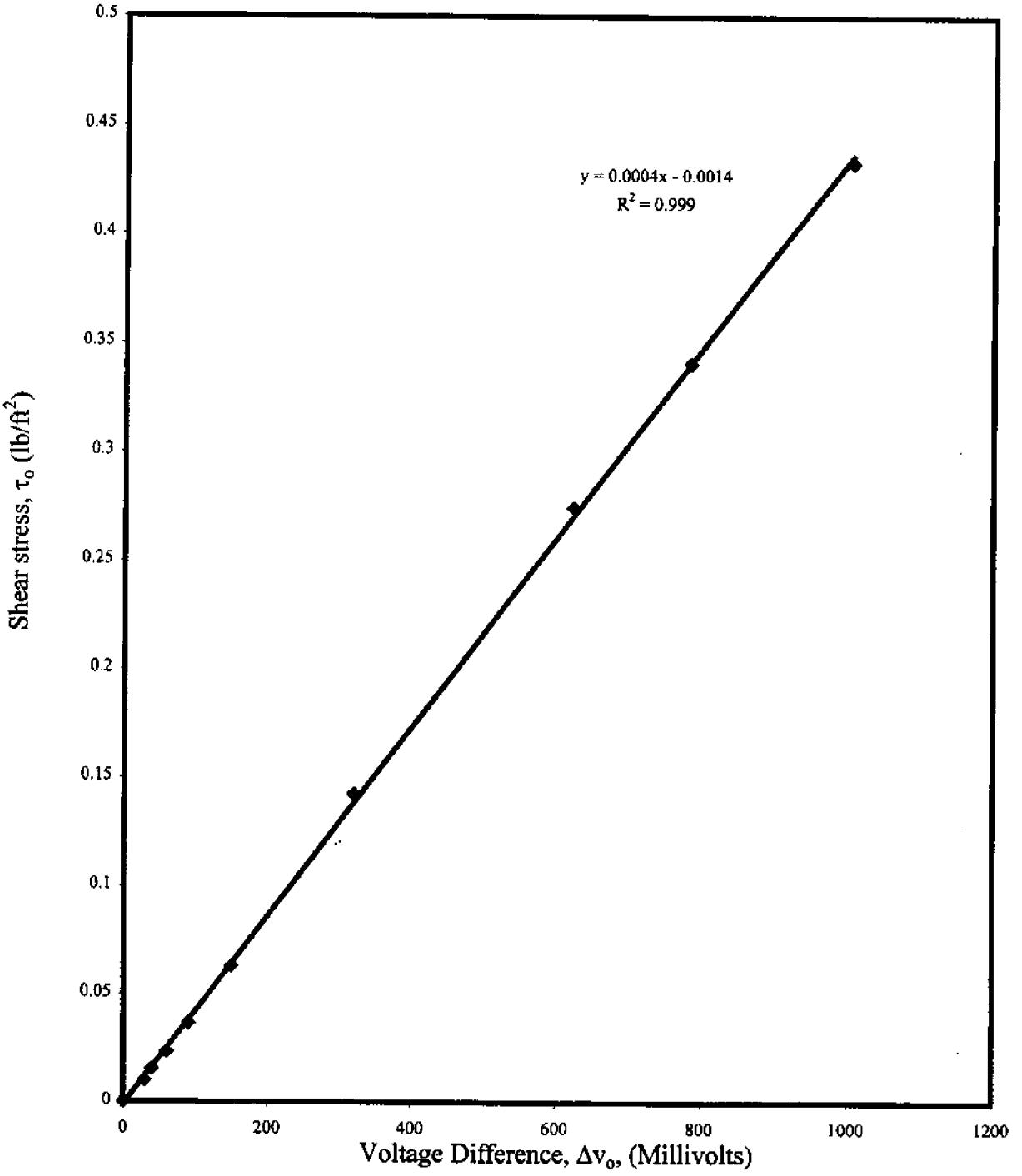

INSTRUMENTAL TESTING

The instrument was tested in the tow tank at UNH as shown in Figure 12. The instrument was towed at four speeds that are representative of the speeds expected in the field. The speeds are shown in Table 4. Three trial runs were performed for each speed. Due to fluctuations during towing an average value of the voltage change was recorded for each run. Then, an overall value of voltage change was obtained for each speed using a given plate (See Figure 13). To determine an average value of shearing stress for each speed, the observed voltage changes were inputted into the calibration equation. Figure 14 shows the relationship between tow speed and shearing stress.

Table 4: Tow Speeds for Tow-Tank Testing of Bottom Drag Meter

Speed 1	0.98 ft/sec
Speed 2	1.38 ft/sec
Speed 3	1.94 ft/sec
Speed 4	2.60 ft/sec

Numerical Analysis of Shear Force on the Flat Plate

To evaluate the accuracy of these measurements, the shear force on the smooth plate was theoretically evaluated using Equations 4 and 5. The water temperature was assumed to be at 60°F. Table 5 shows the discrepancies in shear stress analysis between the measured values and calculated values.

Figure 12: Testing Conditions- Wave Tank & Carriage Appartus

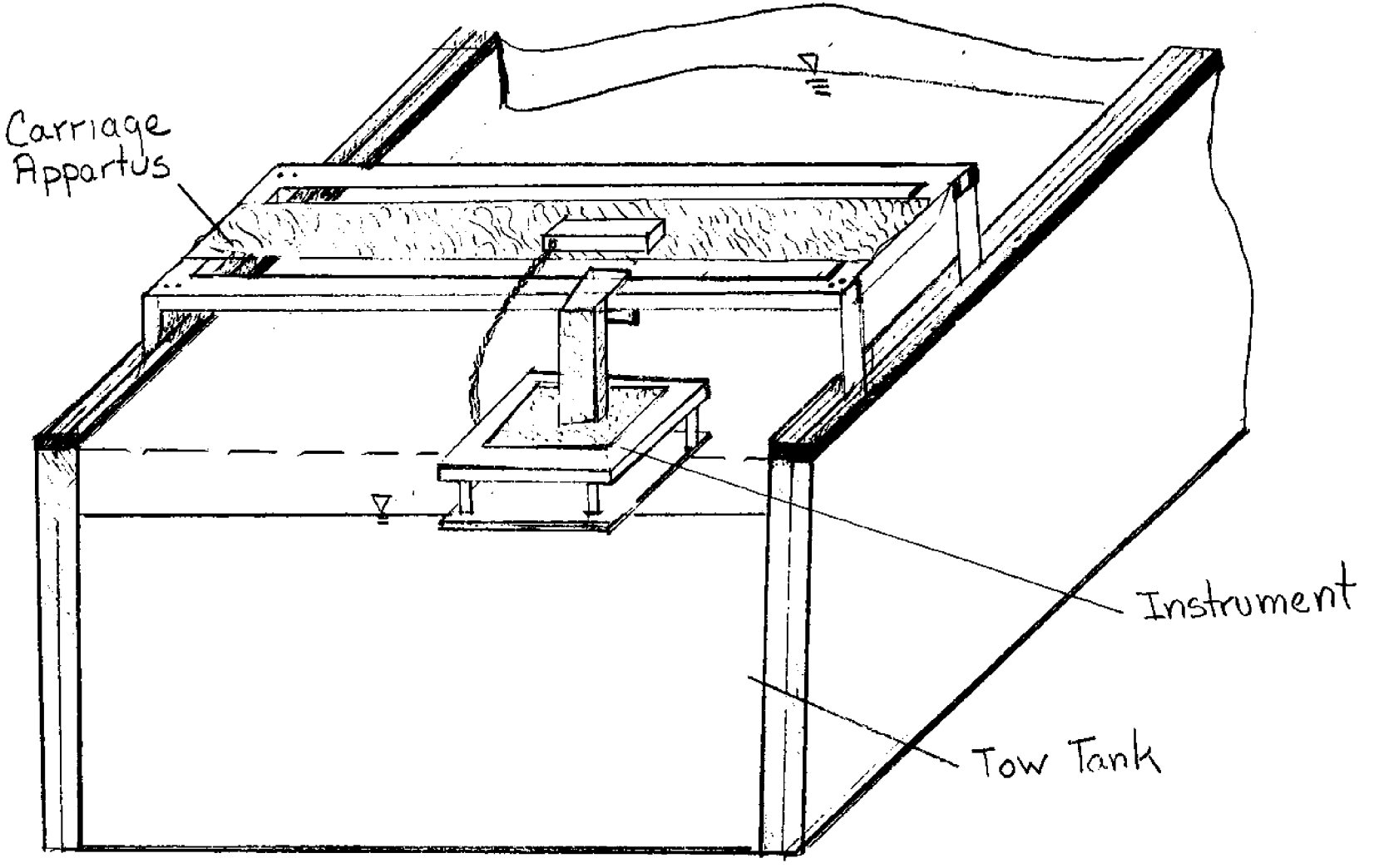

Figure 13: Voltage versus Velocity for Plates with Varying Roughness

(Based on Data Obtained From Instrumental Testing In Tow Tank - Readings are Average Values from Multiple Runs)

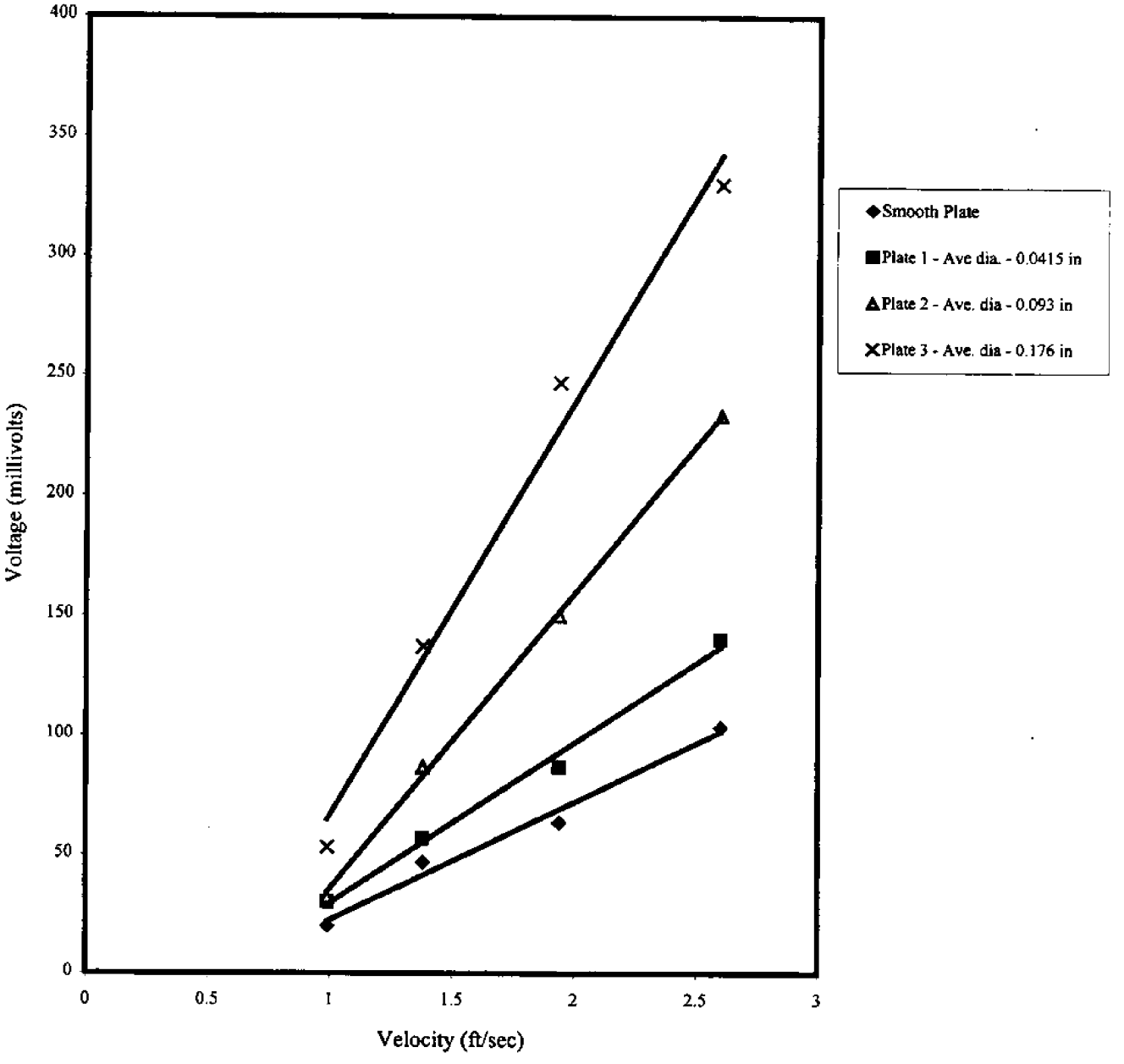

Figure 14: Shear Stress versus Velocity for Plates with Varying Roughness

(Based on Data Obtained From Instrumental Testing In Tow Tank - Readings are Average Values from Multiple Runs)

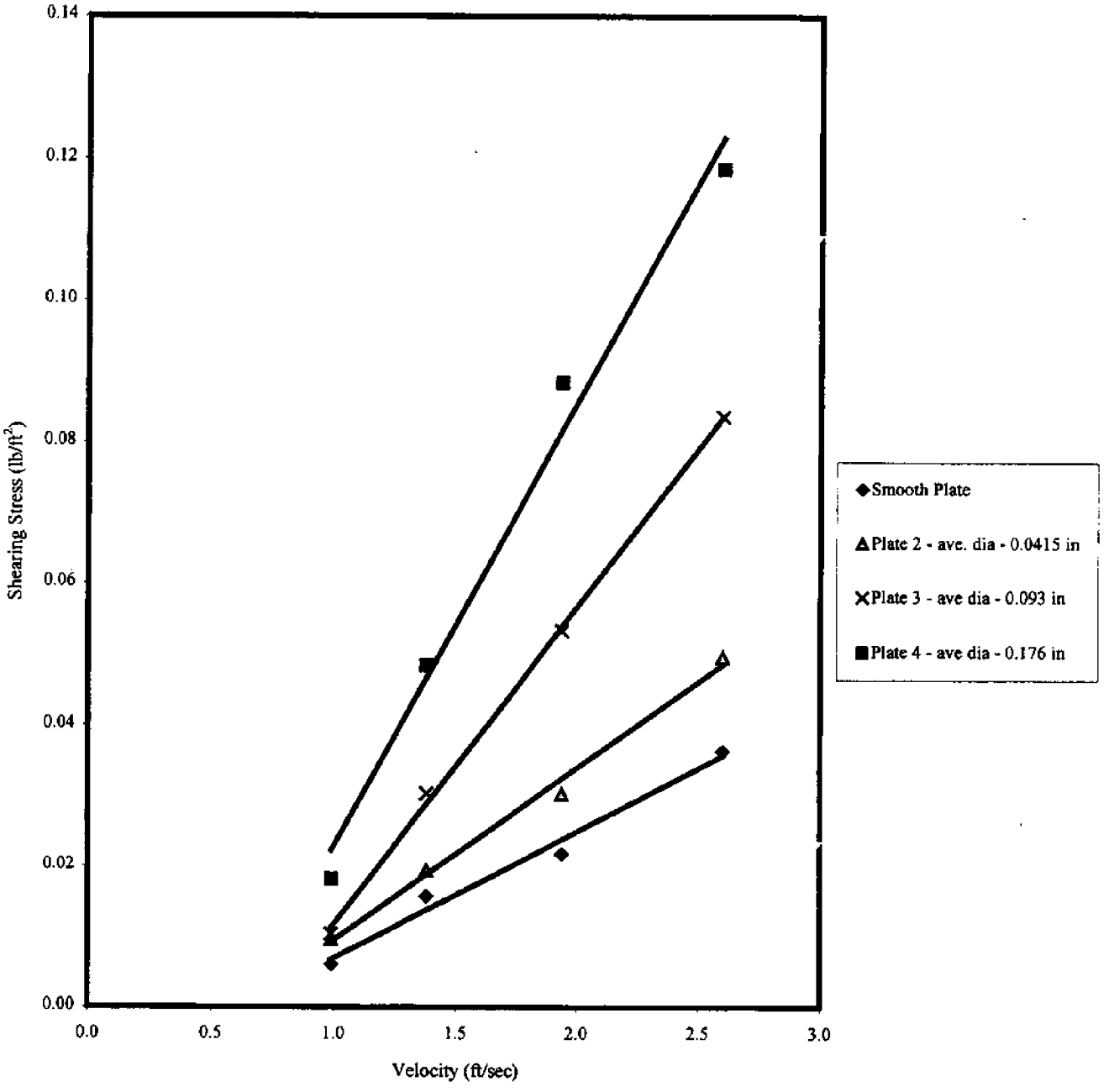

Table 5: Comparison between Observed Values and Calculated Values of Shear Stress on a Smooth Plate

Velocity	Measured Shear Stress	Calculated Shear Stress	Percent Difference
(ft/sec)	(lb/ft^2)	(lb/ft^2)	(%)
0.98	0.007	0.006	15
1.38	0.013	0.016	23
1.94	0.024	0.022	10
2.60	0.041	0.036	12

DISCUSSION AND CONCLUSIONS

Discussion of Observed Data

The data obtained from the calibration process and tow-tests is useful in assessing the instrument's capabilities and limitations in the field. The calibration curve showed a linear relationship between applied stress and voltage difference, Δv_o, over a stress range of approximately 0 to 0.45 lb/ft^2. R^2, was close to one which suggests the calibration equation is a good estimation for stresses within the range tested.

The overall trend of the tow-tests showed increases in velocity are proportional to increases in voltage change. When the values of voltage change were evaluated using calibration equation, a similar relationship between shear stress and velocity was obtained. These tests suggests the instrument will be adequate for correlating increases in shear stress with increases in velocity near the bottom sediments.

During individual tow runs, the voltage readings fluctuated somewhat despite constant velocities. There may be several reasons for these discrepancies.

a. Despite computer controls, the velocity of the carriage during towing may not have been constant.
b. Electronic noise may have interfered with the readings. Signals may have been picked up by the lead wires from electrical devices used for operation of the tow cage or from the voltage supply that operates the amplifier and data logger. Noise effects are most critical when voltage changes are small, as was the case in this experiment.
c. Towing the instrument may have created zones of mixing or variable velocities. Although, the instrument was positioned away from the side walls of the tank, mixing zones due to the existence of the wall may have contributed to the fluctuation in

voltage readings.

Considering these effects, a number of different trials should be performed to obtain an average value of shear stress.

A relationship between shear stress and plate roughness is evident from the results of the tow test. Increases in particle size resulted in increased readings of shear strength. This was similar to Moody's experiments that showed that the friction factor was associated with the relative roughness of pipes (Roberson; Crowe, 1997). Larger size particles have more surface area to interact with the flow and offer more resistance. The relationship was less clear at the lowest tow speed, 0.92 ft/second, as all values appeared very close. Also, the fluctuation in voltage readings during runs was great at this low speed. These two factors may suggest the instrument in not very reliable at speeds less than 1 foot/second.

Comparison between the observed values of shear stress and the calculated values resulted in only a discrepancy of approximately 10 to 20 %. Due to the extremely small values of shear stress that were evaluated, a discrepancy of this nature or greater was expected. This analysis suggests that the strain gages were bonded to the legs correctly such that they experience similar deflections as the legs.

Conclusions

Several of the objectives set forth at the initiation of this project were completed. However, some of the objectives were not meet by the selected design. Furthermore, during construction and testing of the instrument, a few problems and limitations arose that were not anticipated during the design process.

The objectives meet by completion of this instrument are as follows:

A. The instrument does provide a measurement of shear stress that can be used for comparative purpose in the field when velocities near the instrument range from 1 to 3 feet/second. Voltage readings are easily recorded by using the data logger in combination with a computer-graphing program such as EXCEL.

B. The instrument can measure the shear stress at a location close to the sea floor. When seated directly on the sea floor the total height of the instrument is 3.75 inches. However, the addition of the protective sides allows the instrument to be buried such that measurements are taken at 1 inch above the sea floor.

C. The instrument is capable of withstanding the corrosive properties of salt water and the temperature variations expected in the field. Also, several tests were made to ensure that all electrical components are fully protected from the water.

D. The final design required relatively simple metalworking skills and fell well within the allotted budget.

Some of the limitations of the instrument are as follows:

A. Limitations exist in areas of high ambient current. High currents flowing in the same horizontal direction that instrument moves will result in large voltage readings (i.e. large values of shear stress). The instrument may not be able to distinguish from the wave motion from these large current values. Furthermore, extremely high currents may cause overstressing of the legs and damage to the strain gages.

B. To identify the maximum shear stress produced by a wave it is necessary for the instrument to be aligned in the same direction as Jet Ski movement. To ensure this,

one option may be the installation of bright PVC stakes on each side of the instrument and which extend vertically through the water column. These stakes may influence the flow pattern of water beneath the wave. However, this may not be significant if they remain a constant parameter is all analysis.

C. The magnitude of sediment disruption will depend on the method of launching the instrument and/or the possibility of it being buried in the ground. Entirely avoiding disruption to the sediments appeared impossible from all practical standpoints.

D. Values of voltage change recorded in the field can be only compared, if calibration checks are periodically performed. This will consists of performing abbreviated calibrations with known masses and checking to ensure that calibration equations remain constant.

Problems also existed with the design and construction of the physical components of the instrument. For instance, many different types and sizes of hardware were used and most pieces are not interchangeable. Installing or removing the top plate is a little difficult due to the close proximity of the protective walls. Removing the waterproof box and accessing the data logger offers another small challenge - the instrument must be tipped on its side to remove the brackets that hold the data logger in place.

The relatively small values of shear stress, mandated that the legs be extremely thin and narrow. Thus, the legs are also very fragile. Although two screws are used to attach each leg to the bottom plate, only one bolt is used to attach the legs to the top plate. Rough handling easily causes rotation of the legs near the top plate and induces stress in the legs. This may have been avoided by designing each leg such that two bolts could

used to install the top plate.

References

Anderson, Franz. "The Short Term Variation in Suspended Sediment Concentrations Caused by the passage of a Boat Wave Over a Tidal Flat Environment" Department of Earth Sciences, University of New Hampshire and The Jackson Estuarine Laboratory. February 1, 1975

Bower, Joe "Jet Ski Jolt Loons," Audubon Magazine, "September-October 1997, pp 14

Carey, John, "Those #!&#! Jet Skis Roar Up the Potomac", Business Week, September 14, 1998. p. 56.

Dally, J., W. Riley. and K. McConnell, Instrumentation for Engineering Measurements, John Wiley & Sons, Inc. New York, NY, 1993.

Dean, Robert. and Robert A. Dayrymple. Water Wave Mechanics for Engineers and Scientists, Prentice-Hall, Inc., Englewood Cliffs NJ. 1984.

Gorant, Jim, "Jet Bikes Go Green" Popular Mechanics, May 1998. pp. 44-47

Michallet, H and E. Barthelemy. "Experimental Study of Interfacial Solitary Waves", Journal of Fluid Mechanics Volume X, pp 159-177. 1998.

Muir, Wood, Coastal Hydraulics Gorden and Breach Science Publishers., New York, NY. 1969

Myrhaug, Dag, "Bottom Friction Beneath Random Waves", Coastal Engineering. Volume 24, pp 259-273. 1995.

Myrhaug, Dag and Olav H. Slaatelid, and Kostas F. Lambrakos, "Seabed Shear Stresses Under Random Waves: Predictions vs. Estimates From Field Measurements", Ocean Engineering Volume 25, No. 10 pp. 907-916. 1998.

Roberson, John and Clayton T. Crowe, Engineering Fluid Mechanics, John Wiley & Sons, Inc. New York, NY, 1997.

Sharkey, Michael. "Jet Skis Ruining Marshes" The Hampton Union. August 21, 1998

"Students Manual for Strain Gage Technology", Measurments Group, Inc., Raleigh, NC, 1977.

TFX-11 Remote Datalogger/Control Engine User's Guide. Onset Computer Corporation, Bourne MA, 1997.

Williams, Ted. "The Jet Set", Audubon Magazine, July-August 1998, pp 34-39.

NHU-T-99-001 (UNHMP-TR-SG-99-4)

NOTE: A PAGINATION SEQUENCE ERROR WAS MADE IN THIS REPORT.

THERE IS NO PAGE 39 AND 40

Budget

The major components of the budget are shown below. Due to some inexperience with both strain gages and metal working a small percentage of the budget was consumed expenses that aren't necessarily reflected in final instrument.

Item	Cost
Data Logger & Program Information	$500
Gages & Materials Required for Strain Gages	$325
Miscellaneous Items	$45
Waterproof Box	$20
Hardware	$22
Scrap Metal & Sheet Metal	$25
Total Cost	**$940**

Alternative Designs and Disadvantages

Hollow Metal Strip Strain Indicator

- The instrument would be situated upright in the water column so it probably would greatly influence the flow patterns of the water.

- It would be necessary to integrate the readings over the length of the rod to find an approximation of strain. Readings would not be as accurate as desired.

- Making or purchasing a rod flexible enough to deform under the small loads expected would be difficult.

Plastic Ball Strain Indicator

- A large base is required to support the instrument. Installation of this base may significantly disrupt the sediments.

- The drag force on the ball would be easy to calculate. However, accurately relating this force to the force at a location just above the boundary layer would be difficult.

Sliding Plate Force Meter

- Construction of this instrument based upon present metal working skills would be difficult. Many different parts machined parts are necessary.

- Protecting the electrical components from the environment would be difficult. Few materials are both flexible, waterproof, and bond well to metal.

- Restoring the instrument to equilibrium after a wave passed is difficult.

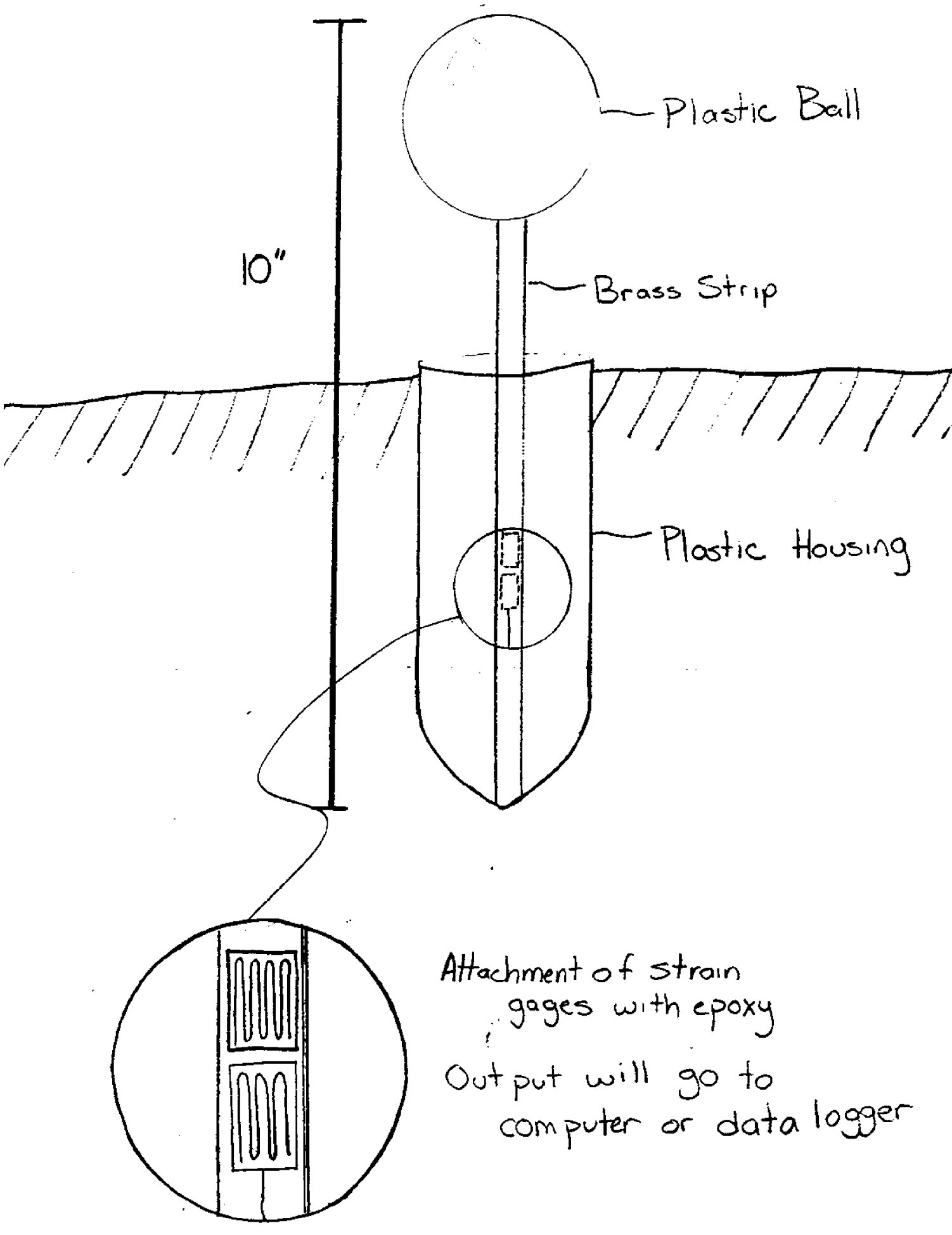
Plastic Ball
10"
Brass Strip
Plastic Housing
Attachment of strain gages with epoxy
Output will go to computer or data logger

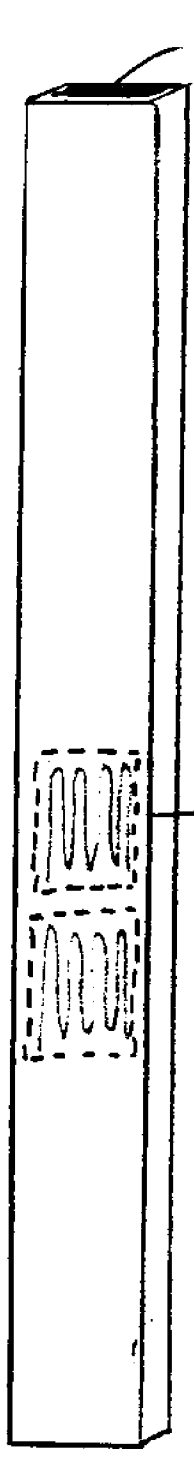
Hollow metal Strip
Strain gages attached on inside
Ends of strip can be welded shut
- Provides nice water proof seal.

Siding Plate Force Meter

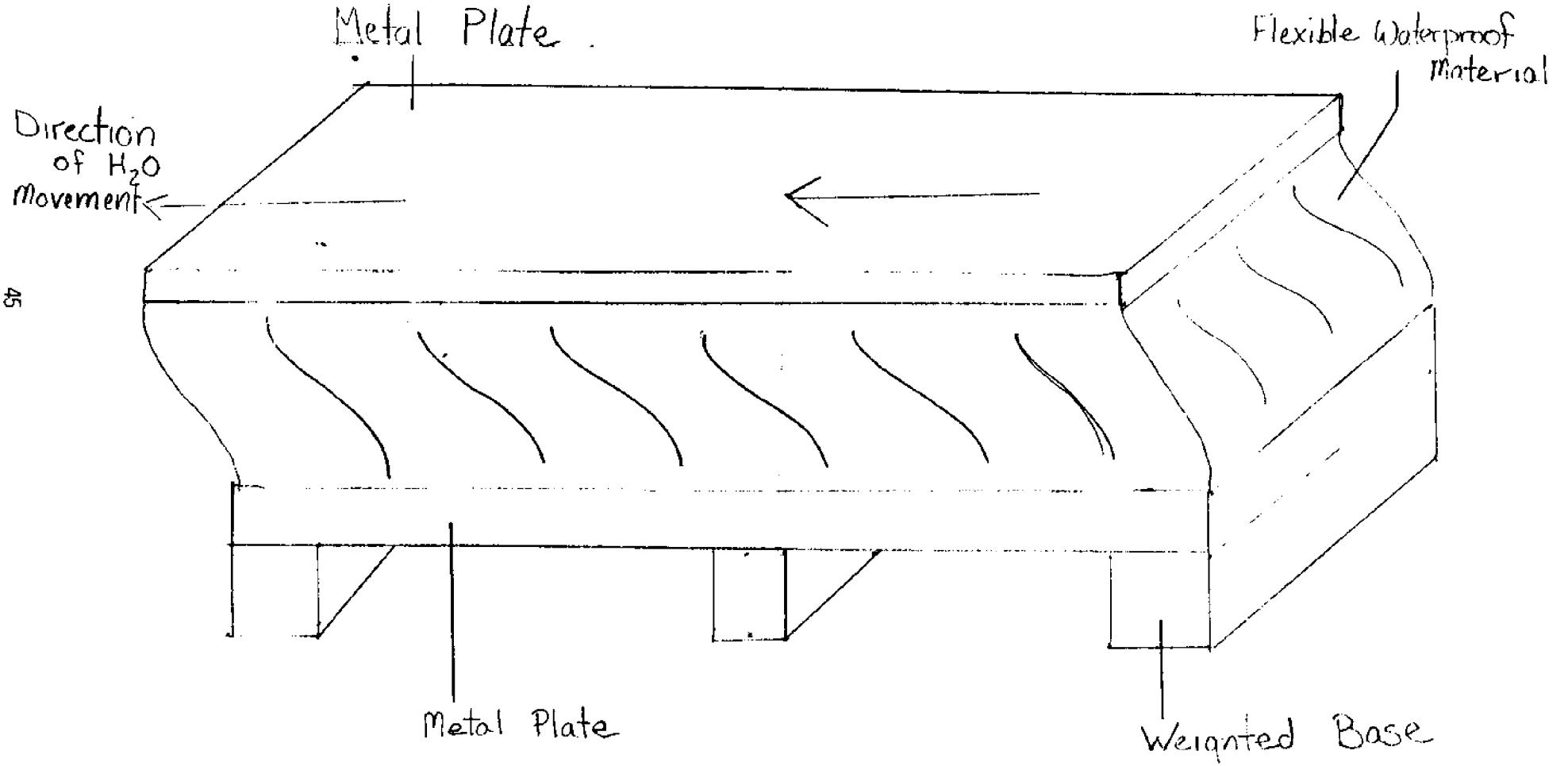

Internal Components - Sliding Plate Meter

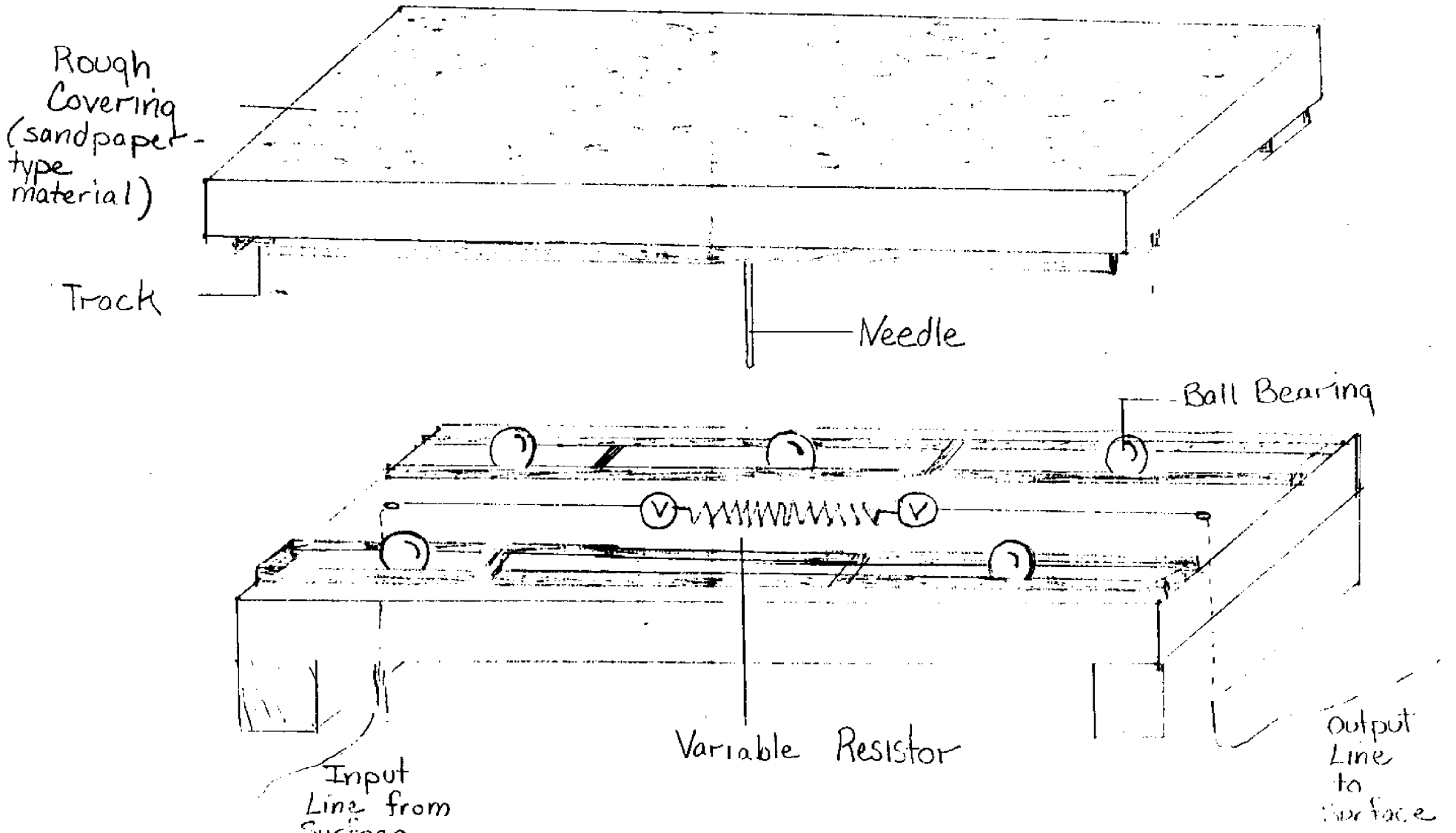

Strain Gage Selection and Installation

With offices throughout the world, Vishay Micro-Measurements Group is the largest manufacture/distributor of strain gages. A comprehensive guide to their services, suggested strain gage applications, and their products is available directly from the company. This section highlights the major factors involved in selecting strain gages and some helpful techniques or methods that were discovered by completing the Bottom Drag Meter Project.

Identify the conditions of which the gage will be used is necessary before selecting a gage.

I. Backing Material– A variety of gage backing options are available. Micro-Measurements designates these by letters E, CE, N2, S2, W, and S. Generally purpose gages used for static conditions, designated by the letter E, have strong, flexible backings but are open-faced (no protective coating over the surface of the gage). The CE gages are also general-purpose gages but work adequately for both dynamic and static stress analysis and have fully encapsulated grids. The other options include thin, high performance film backings for extremely sensitive readings, fully encapsulated gage faces, and/or oversized solder tabs. Experimentation in this project showed that the thickness of the adhesive dictated the sensitivity of the readings, and the backing material appeared to be a minor factor.

II. The foil alloy (resistive material) also can be purchased in a variety of different forms. The self-temperature compensating materials are useful and render temperature corrections/calibrations unnecessary. Micromeasurements, have a

numerical system for selecting gages that correspond to the material they will be used on. Other options include isoelastic alloys that offer longer fatigue lives, materials made specifically for high elongation uses, and materials made for high temperatures, high performance usages.

III. Gage Size – Strain Gages are available in a variety of sizes. The gage length and grid length defines the resistive area of the gage. The matrix width and length define the actual size of the gage with backing material that will be placed on the selected specimen. Narrow, elongated gages are available.

IV. Temperature Range – Most gages are design to operate over the range of -100°F to +350°F. The gages designated by the SK series (S describes the backing material and K defines the foil alloy material) are suggested for temperatures outside of this range.

V. Strain Range – The general purpose gages, CE and E, have the highest range of strain: approximately +-3%. Other gages have ranges around +/1.5%.

VI. Mode of Strain – Gages are available to measure strain in up to four directions. Stacked rosettes are available that have strain elements situated at 45° or 60° from one another. Also, two element rosettes are available that are situated at 90° from one another. These configurations are valuable in for materials placed under biaxial or triaxial stress. An example may be a metal rod placed in torsion.

VII. Useful Options – A variety of options exist to protect the gages or aid in the attachment of leadwires. One the most useful discovered during this project are the jumper cables extending from the gage tabs to larger external soldering tabs. This eliminates the delicate process of soldering wires to the tiny tabs. Also larger, more

manageable wires can be attached to the external soldering tabs. The other valuable option was the pre-attachment of lead wires. Gages with this option generally cost twice as much. For this instrument, this option proved to be worthwhile.

VIII. Special Purpose Sensors – Specific gages are manufactured to aid in research. Examples include: strip gages for strain gradient investigations, gages to be use in magnetic fields, and crack propagation gages. Micro-measurements or another manufactured should be consulted for complete details.

Procedure for attaching Strain Gages

Micro-Measurements provides a comprehensive guide to strain gage adhesion and surface preparation. They also sell a variety of instruments, tools, and adhesives.

Preparation of the Surface

I. Degreasing the Surface – The micro-measurement brand degreaser is a chlorinated hydrocarbon solvent available in a pressurized can. The solvent should be sprayed onto a gauze sponge and used to wipe the workpiece surface in one direction only. The gauze should be disposed of to prevent cross-contamination. No experimentation on other degreasing products was performed for comparison between brands, however, some technicans recommend isopropyl alcohol (rubbing alcohol). Store-bought gauze worked well.

II. Conditioning the Surface

A. Conditioner – A mild phosphoric acid is sold in convenient dispensors by Micro-measurements to etch the work surface. Again, wipe the surface in one direction and discard the guaze upon completion.

B. Neutralizer – Micromeasurements offers an ammonia-based neutralizer to raise the pH and stop any chemical reactions that occurred between the conditioner and surface.

III. Abrading the Surface – For optimal adhesion the working surface should be slightly abraded. Silicon-Carbide paper is sold by Micro-measurements in 220 and 320 grits for steel surfaces and 320 grit for softer metals. Similar paper was obtained from the local hardware store and worked adequately. If the gage requires protective coating, it may be advantageous to abrade a large surface so that the protective coating also bonds well. Gages should be adhered to metal materials shortly after abrading the surface because chemical reactions between the abraded metal and the air may alter the strength capabilities of the adhesive. (This is especially true for brass.)

IV. Adhesive Materials – A variety of different adhesives are sold by Micro-measurements that offer different levels strength and curing rates. M-Bond AE-10, a general purpose, room-temperature-curing adhesive, was used in this project. It is available in bulk or in kits that come with 10 gram mixing jars and curing agent. A considerable amount of the mixed adhesive was wasted because only four gages were attached at once. Thus, for small applications, the kits are not recommended. The adhesive was fairly viscous and spreading only a thin coat onto the gage surface was difficult. Super glue, a fairly well accepted strain gage adhesive for general purposes, was also experimented with during this project. It resulted in a much thinner layer of adhesive and offered quicker curing times.

Under extreme conditions it is best to consult the manufacture for adhesive selection.

V. Gage Installation – The adhesive should be spread onto the back of the gage. While adhering the gage to the working surface, it is important to avoid overstressing the gage by accidentally bending it. A small surgical scalpel or putty knife is useful for applying the adhesive and tweezers help hold the gage in place. Slight pressure should be applied to the gage until the adhesive appears tack-free.

VI. Attaching Lead Wires – As described in the Strain Gage Selection Section - Part VII a variety of useful options are available to aid in this process.

A. Materials – Micro-Measurements sells a variety of different wires, cables, and soldering supplies. The most essential supplies are solder, flux, rosin solvent, and a soldering iron (Most of these are available from a general hardware supplier). The solder should be small in diameter and composed of tin, silver, and/or antimony.

B. Process - The majority of soldering tabs are very small, so it is best to run small wires from the tabs to external tabs. The soldering iron should be set at approximately 550°F – 600°F. All wires should be cut to the same size to minimize error due to unequal wire resistance. The tips of the wires should be "tinned" by touching the solder-coated iron to them. Once the wires are positioned, the solder-coated iron can again be touched to the wires so that a small round bead of solder is deposited on the surface. An irregular sized bead is a sign of uncompleted solder. Flux is used to promote the flow of the

solder once heat is applied. Rosin solvent can be used to clean up any extra or misplaced solder.

VII. Protective Coatings - A variety of different coatings are available from Micro-Measurements to prevent strain gage degradation by moisture, chemical attack or mechanical damage. Also, various epoxies, available from manufactures such as GE Silicones, may provide adequate protection but should be tested. Micro-Measurements also provides detailed procedures for various environmental conditions. The procedure for gages submerged in marine waters was followed during the construction of the first prototype in this project. The adhesive recommended, M-J Coat, is available in ready-to-mix containers. A significant amount of the expensive adhesive was wasted, so, other products were experimented with.

Check to ensure that strain gages will not be deformed by excessive strains

*Maximum allowable strain is 3%

Dimensions of Top Plate

$L := 1.166\ ft$
$B := 0.833\ ft$

Properties of Salt Water at 50°F

Definition $slug := 1\ lb$

Density $\rho := 1.99\ \frac{slug}{ft^3}$

Kinematic Density $\nu := 1.5 \cdot 10^{-5}\ \frac{ft^2}{sec}$

Dimesions of each Leg

Distance to gage	$x := .166$	
Width of leg	$b := .03333$	All dimensions in feet
Thickness of leg	$w := 8.333 \cdot 10^{-4}$	
Modulus of Elasticity	$E := 2.16 \cdot 10^{9}\ \frac{lb}{ft^2}$	

Evaluation of Largest Strain (ε) using largest expected velocity, u_{max} = 3 ft/sec

Definition of Strain

$$\varepsilon := 6 \cdot \frac{\frac{F_d}{4} \cdot x}{E \cdot b \cdot w^2} \quad \text{where} \quad F_d := \frac{u_{max}^2}{2} \cdot B \cdot L \cdot \rho \cdot C_f$$

Drag Force

$$C_f := \frac{.074}{Re_{max}^{\frac{1}{5}}}$$

Coefficient of Friction for Turbulent Flow

$$Re_{max} := \frac{u_{max} \cdot L}{\nu}$$

Reynolds Number based on the Length of the Flow

So analysis of u_{max} = 3 ft/sec shows:

$u_{max} := 3\ \frac{ft}{sec}$

$Re_{max} := \frac{u_{max} \cdot L}{\nu}$ $\quad Re_{max} = 2.332 \cdot 10^5$

$$C_f := \frac{.074}{Re_{max}^{\frac{1}{5}}} \qquad C_f = 6.247 \cdot 10^{-3}$$

$$F_d := \frac{u_{max}^2}{2} \cdot B \cdot L \cdot \rho \cdot C_f \qquad F_d = 0.054 \quad lbf$$

$$\varepsilon := 6 \cdot \frac{\frac{F_d}{4} \cdot x}{E \cdot b \cdot w^2} \qquad \varepsilon = 2.706 \cdot 10^{-4}$$

Expected Strain with a Velocity of 3 ft/sec

Thus, these dimensions in conjuction with the expected forces should not over strain the gages

Program Derived to Order Data Logger to Begin Sampling

Task

Part 1

Sleep 0 — *Set the default time to 0.*

Repeat — *Start checking switch..*

Sleep 300 — *Run this part of the program every 300 units or 3 seconds (1 unit = .01 second .*

Pset 23 — *Send +5 volts to the switch from pin 23.*

Record = Pin (22) — *Record value of pin 22. If switch is on it is connected to pin 23 and is a +5 volts. If switch is off then pin 22 is connected to ground and is 0.*

Pclr 23 — *Stop sending voltage at pin 23.*

Until record > 3 — *If receiving a voltage supply from pin 23 greater than 3 volts than move to part 2 of the program and begin recording data. If less than 3 volts than continue to check switch. (Three volts was arbitrarily chosen because it was between 0 and 5.)*

Part 2

Sleep 0 — *Set the default time to 0 seconds*

Repeat

Sleep 10 — *Run this part of the program every .1 seconds*

Bottom = !float (chan (18)) — *Check channel 18 – Output voltage from amplifier*

BigStr$ = str ("", #6.2F, bottom) — *Save data in a string, BigStr. #6.3F defines the number of decimal places the data logger must record. In this case it was set at .01 Volts or 10 mV.*

Store BigStr$ — *Stores String.*

Pset 23 — *Send +5 volts to pin 23.*

Figure 1A: Relationship between Voltage Change and Velocity for the Smooth Plate

(Instrument Tested in Tow Tank on April 16, 1999. Voltage Readings are Average Values for Multiple Runs)

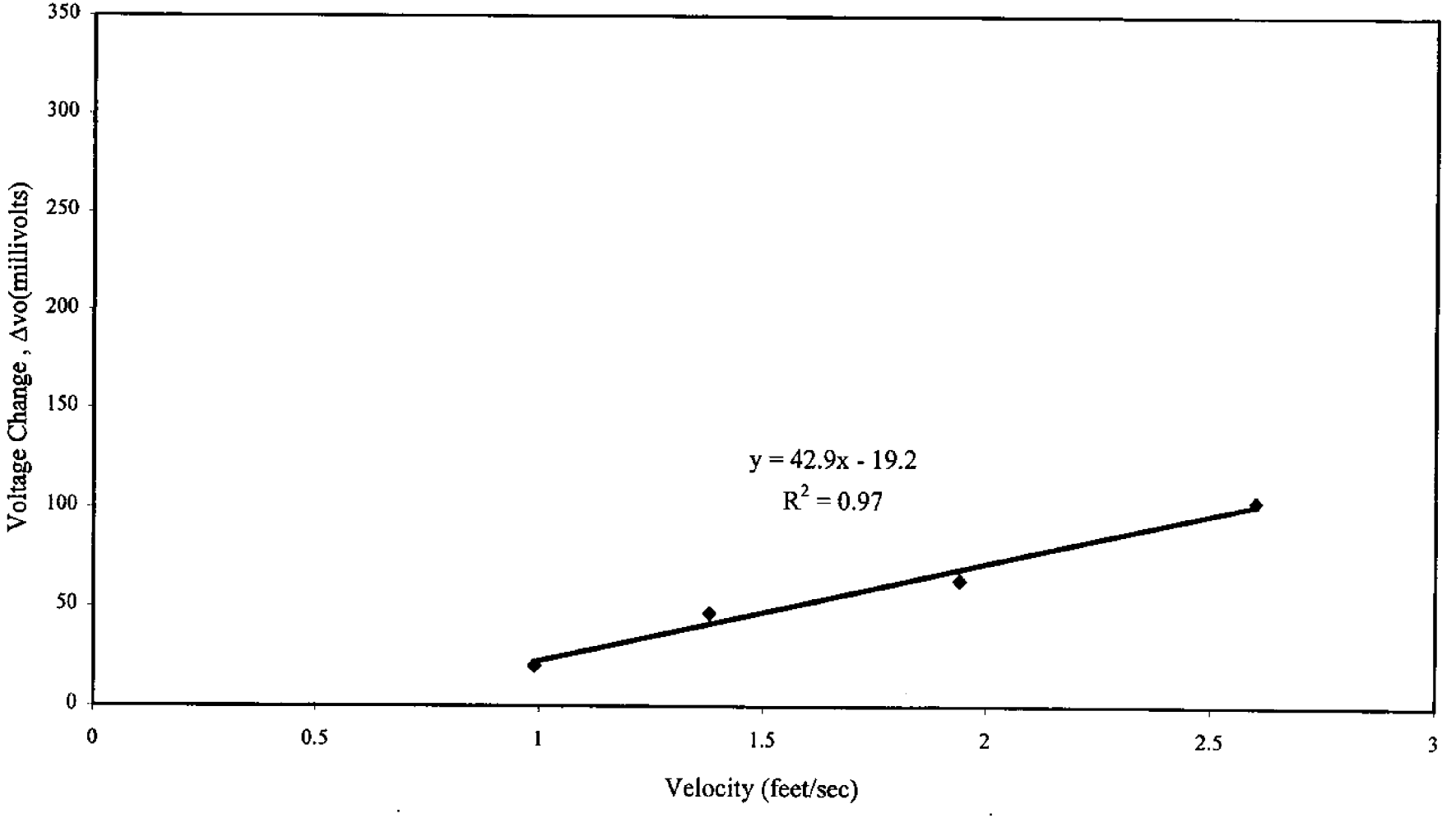

Figure 2A: Relationship between Voltage Change and Velocity for Sand Coated with Average Particle Diameter of 0.0415 Inches

(Instrument Tested in Tow Tank on April 20, 1999. Voltage Readings are Average Values from Multiple Runs)

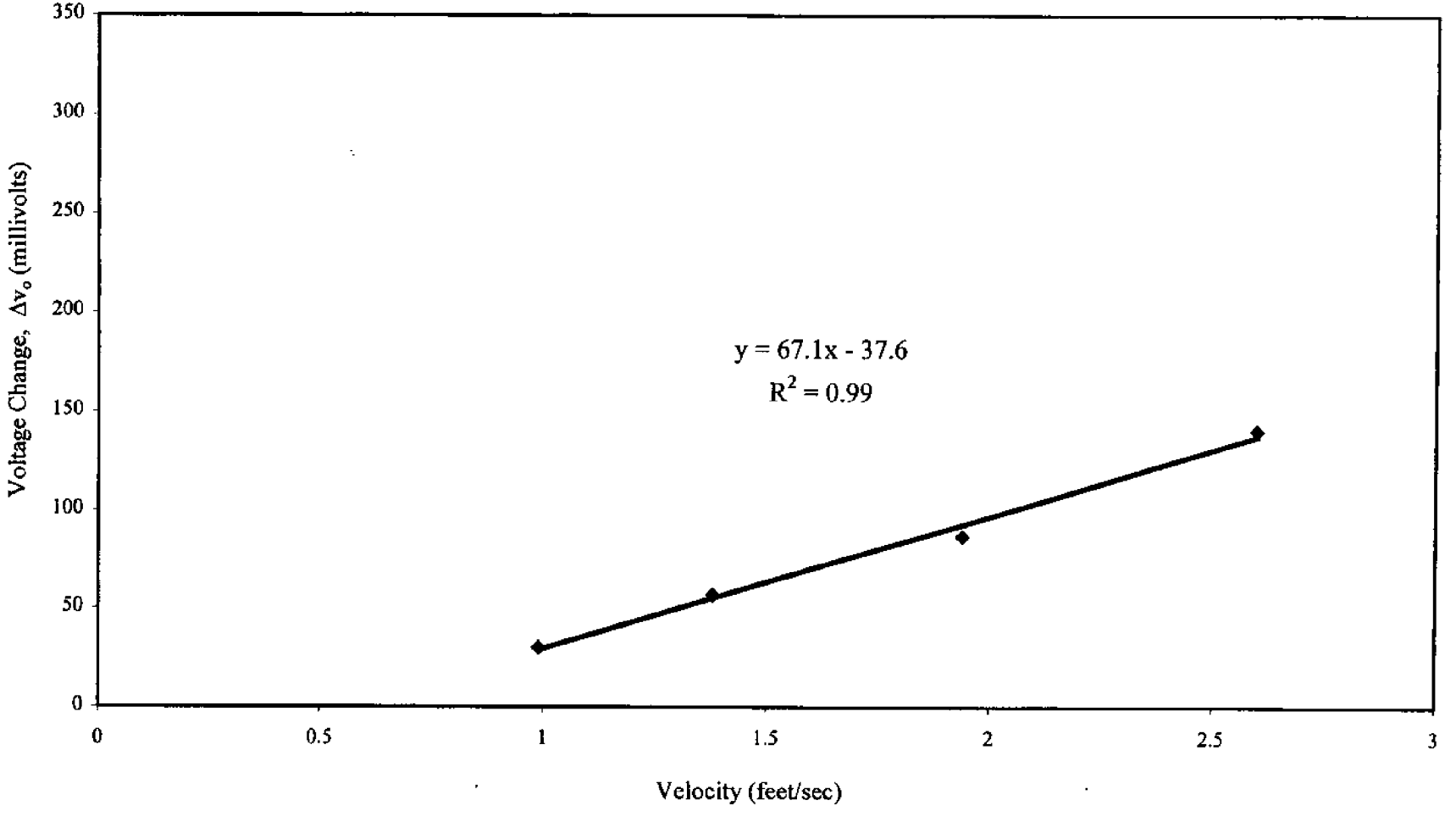

Figure 3A: Relationship between Voltage and Velocity Using Sand Coated Plate with Average Particle Diameter of 0.093 Inches

(Instrument Tested in Tow Tank on April 16 - Voltage Readings are Average Values from Multiple Runs)

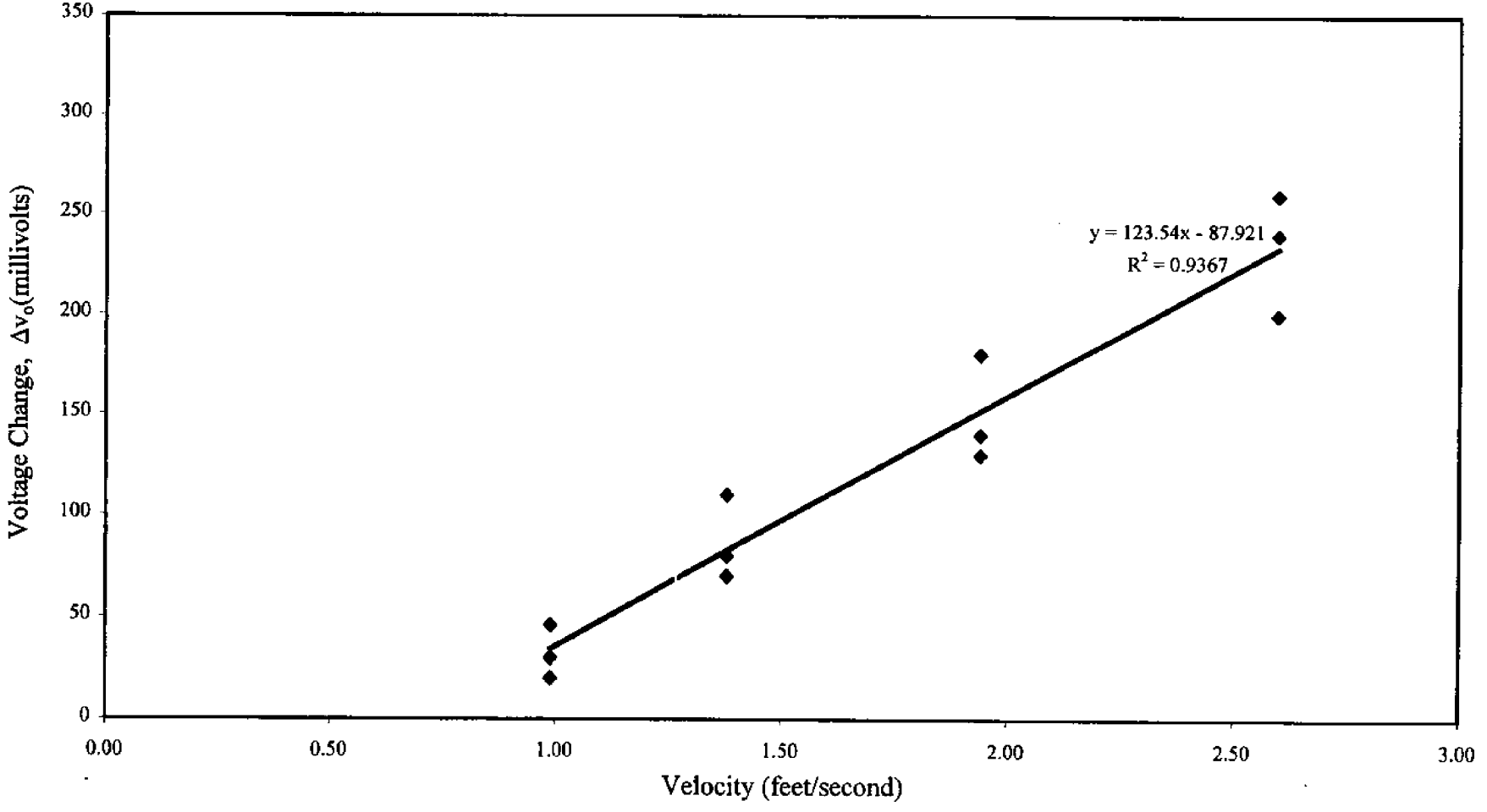

Figure 4A: Relationship between voltage change and velocity for Sand Coated Plate with an Average Particle Diameter of 0.176 Inches

(Instrument Tested in Tow tank on April 20, 1999. Voltage Readings are Average Readings Obtained from Multiple Runs)

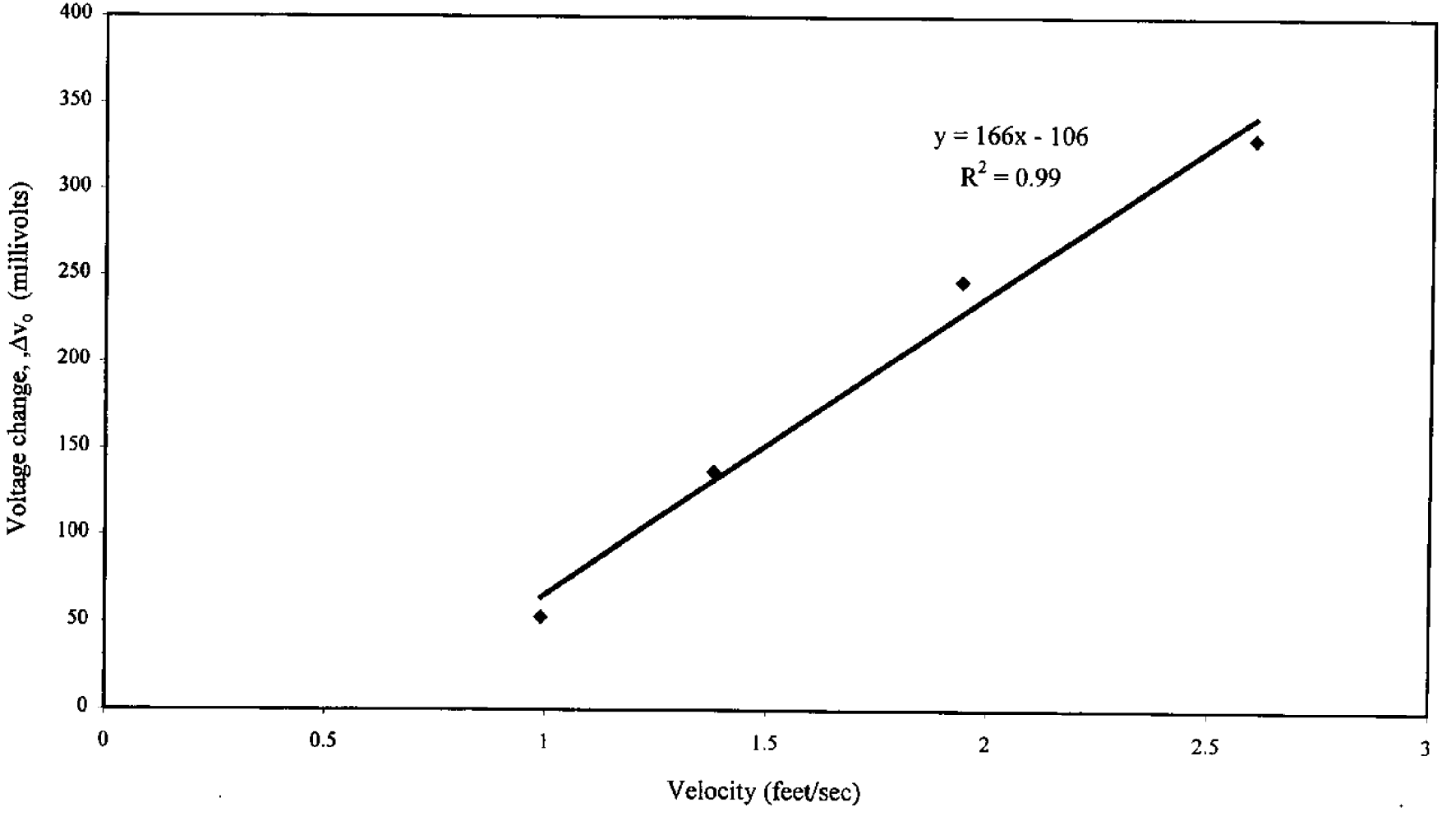

Figure 5A: Relationship Between Shearing Stress and Velocity for Smooth Aluminum Plate
(Data Based on Test Conducted Using the Instrument in the Tow Tank on April 16, 1999)

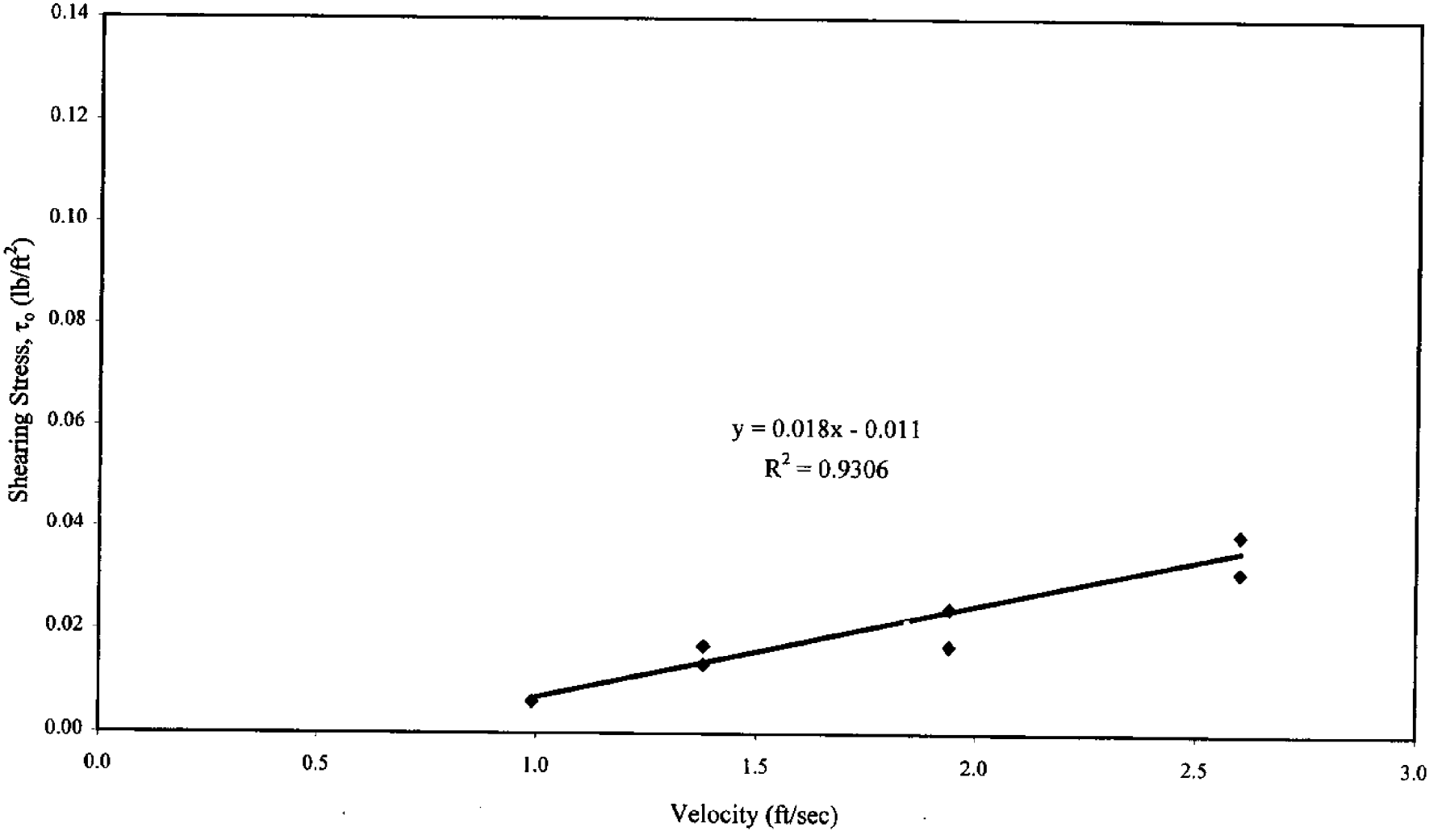

Figure 6A: Relationship Between Shearing Stress and Velocity for Sand Coated Plate with an Average Diameter of 0.0415 Inches

(Data Based on Test Conducted Using The Instrument in the Tow Tank on April 16, 1999)

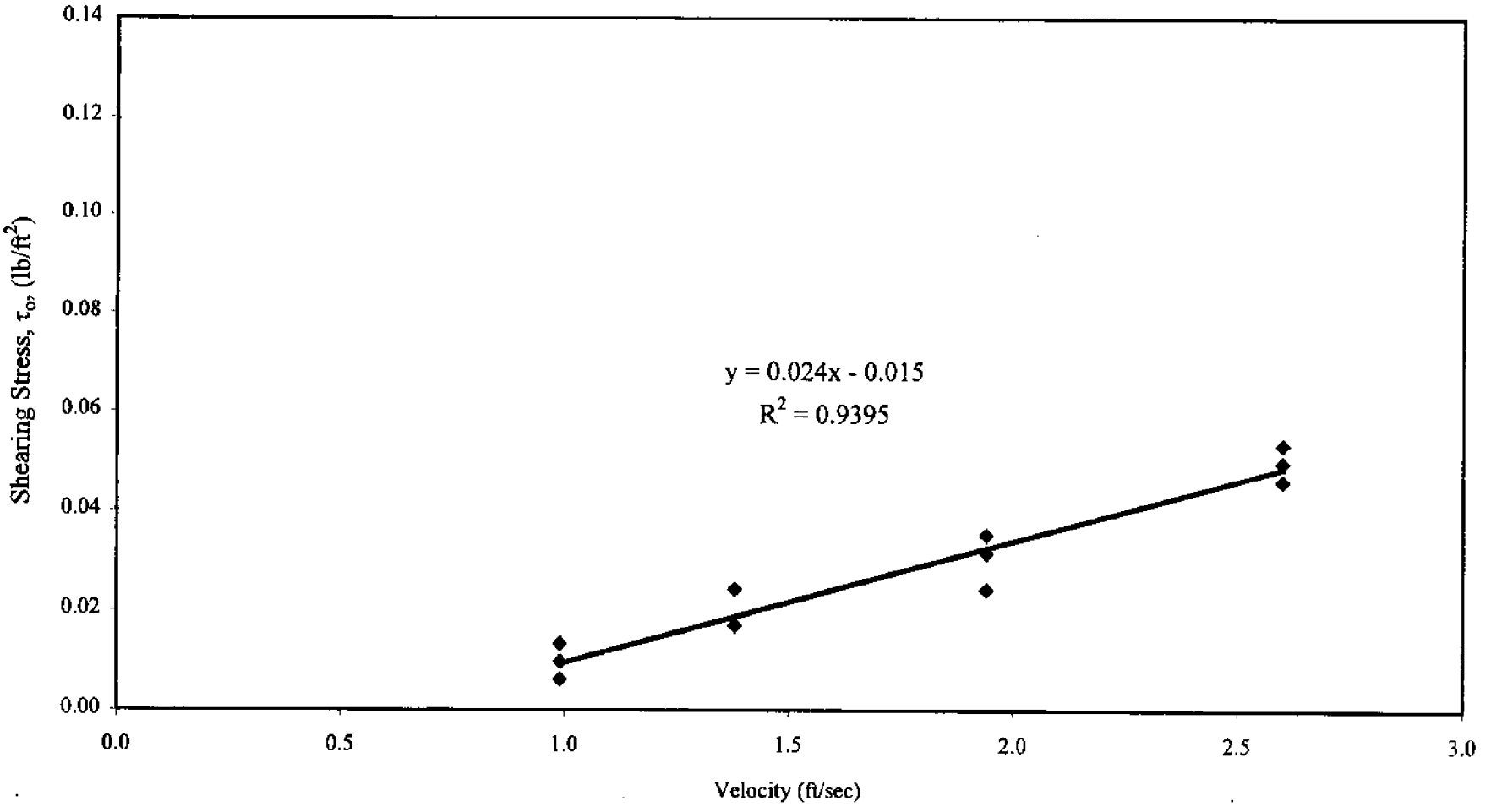

Figure 7A: Relationship Between Shearing Stress and Velocity for Sand Coated Plate with an Average Diameter of 0.093 Inches

(Data Based on Test Conducted Using The Instrument in the Tow Tank on April 20, 1999)

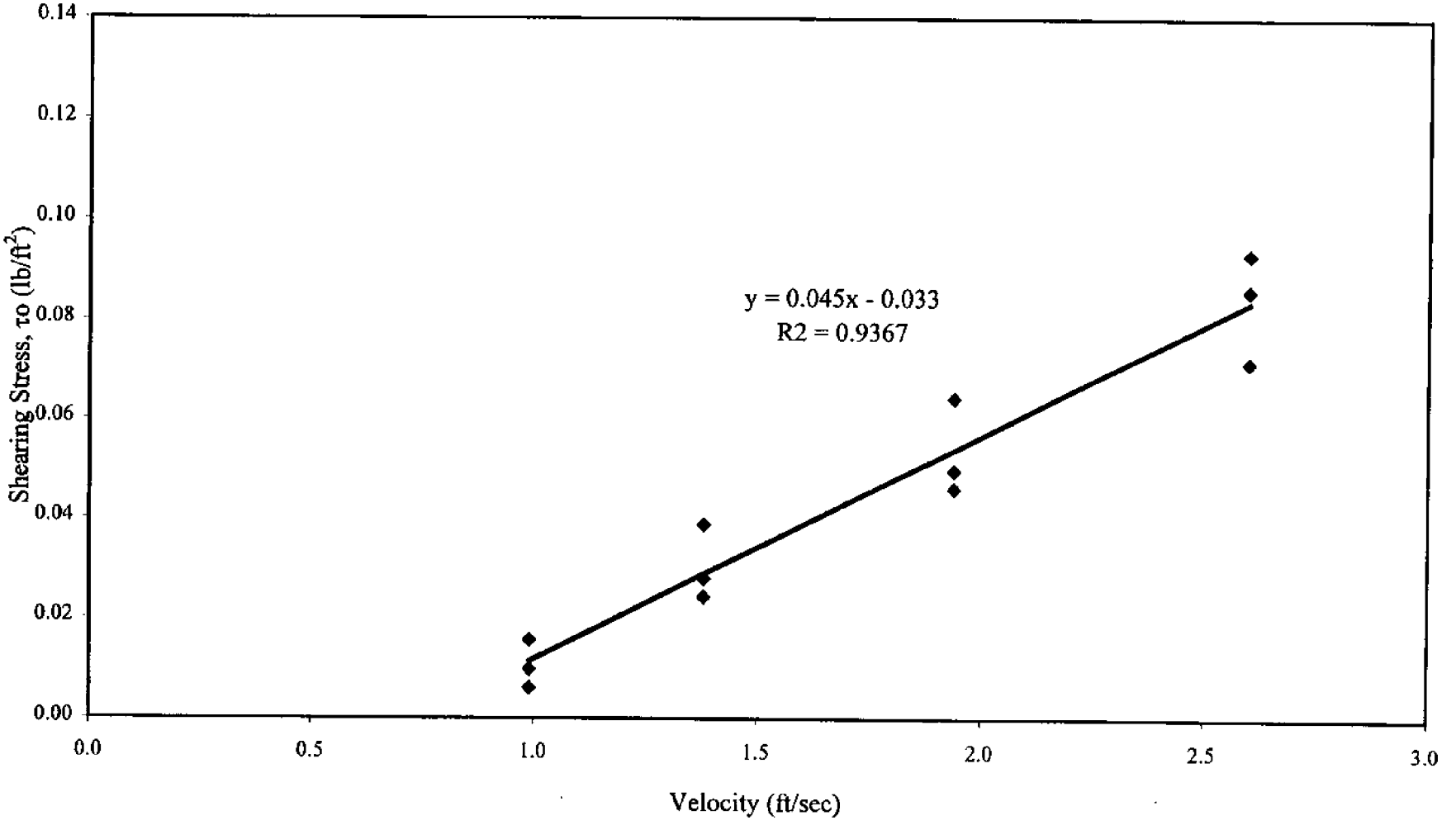

Figure 7A: Relationship Between Shearing Stress and Velocity for Sand Coated Plate with an Average Diameter of 0.176 Inches

(Data Based on Test Conducted Using The Instrument in the Tow Tank on April 20, 1999)

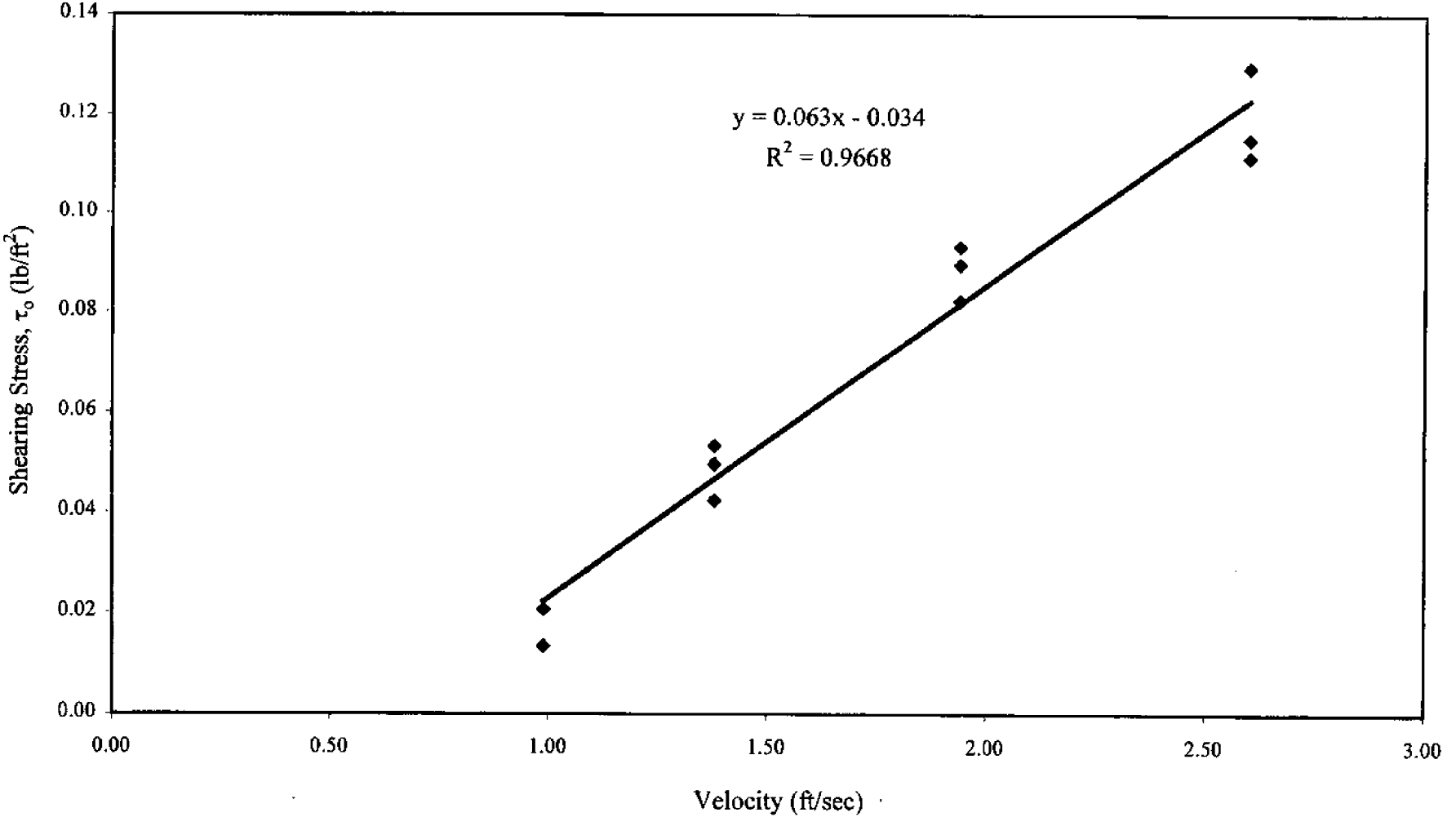

Table A1: Test Data for Smooth Plate

Velocity (ft/sec)	Initial Voltage Readings (Volts)	Average Voltage Readings During Run (Volts)	Voltage Difference (Volts)	Voltage Difference (Millivolts)	Shearing Stress (lb/ft^2)
0.99	1.36	1.34	0.02	20	0.006
0.99	1.36	1.34	0.02	20	0.006
0.99	1.36	1.34	0.02	20	0.006
1.38	1.35	1.4	0.05	50	0.017
1.38	1.35	1.39	0.04	40	0.013
1.38	1.35	1.4	0.05	50	0.017
1.94	1.36	1.41	0.05	50	0.017
1.94	1.36	1.29	0.07	70	0.024
1.94	1.36	1.43	0.07	70	0.024
2.60	1.36	1.45	0.09	90	0.031
2.60	1.36	1.47	0.11	110	0.039
2.60	1.36	1.25	0.11	110	0.039

Table A2: Test Data for Plate 2 with Average Particle Diameter of 0.0415 Inches

Velocity (ft/sec)	Initial Voltage Readings (Volts)	Average Voltage Readings During Run (Volts)	Voltage Difference (Volts)	Voltage Difference (Millivolts)	Shearing Stress (lb/ft^2)
0.99	1.33	1.35	0.02	20	0.006
0.99	1.34	1.37	0.03	30	0.010
0.99	1.34	1.38	0.04	40	0.013
1.38	1.33	1.28	0.05	50	0.017
1.38	1.34	1.27	0.07	70	0.024
1.38	1.36	1.31	0.05	50	0.017
1.94	1.33	1.26	0.07	70	0.024
1.94	1.34	1.44	0.1	100	0.035
1.94	1.34	1.43	0.09	90	0.031
2.60	1.34	1.48	0.14	140	0.050
2.60	1.33	1.2	0.13	130	0.046
2.60	1.34	1.19	0.15	150	0.053

Table A3: Test Data for Plate 3 with Average Particle Diameter of 0.093 Inches

Velocity (ft/sec)	Initial Voltage Readings (Volts)	Average Voltage Readings During Run (Volts)	Voltage Difference (Volts)	Voltage Difference (Millivolts)	Shearing Stress (lb/ft^2)
0.99	1.35	1.32	0.03	30	0.010
0.99	1.34	1.32	0.02	20	0.006
0.99	1.39	1.34	0.05	46	0.016
1.38	1.34	1.42	0.08	80	0.028
1.38	1.33	1.40	0.07	70	0.024
1.38	1.34	1.23	0.11	110	0.039
1.94	1.34	1.20	0.14	140	0.050
1.94	1.34	1.21	0.13	130	0.046
1.94	1.34	1.52	0.18	180	0.064
2.60	1.34	1.60	0.26	260	0.093
2.60	1.34	1.58	0.24	240	0.086
2.60	1.34	1.14	0.20	200	0.071

Table A4: Test Data for Plate 4 with Average Particle Diameter of 0.176 Inches

Velocity (ft/sec)	Initial Voltage Readings (Volts)	Average Voltage Readings During Run (Volts)	Voltage Difference (Volts)	Voltage Difference (Millivolts)	Shearing Stress (lb/ft^2)
0.99	1.36	1.32	0.04	40	0.013
0.99	1.35	1.29	0.06	60	0.021
0.99	1.35	1.41	0.06	60	0.021
1.38	1.36	1.51	0.15	150	0.053
1.38	1.35	1.49	0.14	140	0.050
1.38	1.36	1.24	0.12	120	0.042
			0		
1.94	1.36	1.62	0.26	260	0.093
1.94	1.35	1.6	0.25	250	0.090
1.94	1.36	1.13	0.23	230	0.082
2.60	1.36	1.05	0.31	310	0.111
2.60	1.35	1.71	0.36	360	0.129
2.60	1.36	1.68	0.32	320	0.115